NTNU
Norwegian University of
Science and Technology

Experiments on ion exchange membrane

Ramn Erstad

Chemical Engineering and Biotechnology
Submission date: June 2017
Supervisor: Heinz A. Preisig, IKP

Norwegian University of Science and Technology
Department of Chemical Engineering

Preface

This masters thesis was written in 2017 at the process systems engineering group at the department of chemical engineering at NTNU. This was the last obstacle on my way to a final degree.

I would like to thank my supervisor Heinz A. Preisig for his supervision during this year's thesis and the master project last autumn. Much credit must be given to my co supervisor Cansu Birgen for her handling of various problems which occured with the lab and the setup and interesting discussions about the results when they showed up. A great thanks to Arne Tobias Elve and Sigve Karolius for their help whenever a computer programme did not choose to work, which was most of the time. And the guy from Sintef who finally managed to fix the data logging.

I would like to thank my classmates with whom I have worked alongside for the last year.

I would like to thank my sweet peas plant for all the great moments we have spent together, I am sorry that people try to kill you all the time, but you are simply the only thing of value ever produced in this office. The ghost cat Findus deserves a lot of credit for bringing a tapas buffet and his mental support.

My mother deserves a great deal of credit for taking the time to read through all of these pages and her input was greatly appriciated and to my brother who helped me set the important goals during this period. And to the rest of my family.

Declaration of compliance

I hereby declare that this thesis is an independent work in agreement with the exam rules and regulations of the Norwegian University of Science and Technology.

Ramn Erstad
Trondheim 15.06.2017

Abstract

To achieve the goal of increasing the amount of biofuels, esters with their acid and alcohol components made from lignocellulose can be a sustainable technology. The maximal achievable concentration of carboxylic acids from a fermentation process is low and without an effective means of separation this is not a viable economic option compared to production from petrochemicals. To date the most promising technique for separation is membrane electrodialysis. This technique allows the removal of the acids without harming the fermentation stock.

In this master project experiments on an electrodialysis membrane has been designed and the setup and design have been adjusted to each other in order to run the experiment. The design was made to explore a large part of the possible operational area to recommend areas to be further researched. A factorial design was chosen due to the large amount of information given by the few number of experiments. The goal was to see the effects of electrical current and the concentration of acetic acid on different performance indicators. This included the temperature, pH, coulombic efficiency, yield, acetate removal rate and removal time. To analyse the performance different online measurements techniques were applied these included pH, temperature and electrical potential and current logging. Samples from the experiment were analysed by HPLC and analysis of variance was performed on these results to check for any correlations and discover how the system might evolve.

The analysis of variance showed that the experimental variables had a significant effect on the Coulombic efficiency and rate of transfer. For both of them, the interaction had a significant effect. The results from the analysis of variance indicated that the best operating conditions were at a high concentration and a strong electrical current. This operational mode had a lower electrical resistance during four hour runs indicating that the optimal economical performance is situated in the same area. The yield showed no significance. The catholyte pH increased in all experiments and reached a steady state around pH 12.5 while the anode pH remained constant. The temperature for both compartments increased because of the electrical resistance.

Samandrag

For å oppnå målet om økte mengder biodrivstoff, esterar med syre og alkohol komponentar frå lignocellulose kan vere ein bærekraftig teknologi. Den maksmimalt oppnåelege konsentrasjonen av karboksylsyrer i ein fermenteringsprosess er låg og utan effektive separasjonsteknikkar ikkje konkurransedyktig mot petrokjemikaliar. Til dags dato den mest lovande teknikken er membranelektrodialyse. Den gjennomfører separasjonen utan å skade mikroorganismane.

I denne masteroppgåva vart eksperiment på ein elektrodialysemembran utforma and oppsettet og utforminga vart tilpassa kvarandre, slik at eksperimentet kunne verte gjennomført innan begges rammer. Utforminga var skapt for å utforske ein stor del av det moglege operasjonsområdet, for å dermed framstille område for vidare utforskning. Faktoriel utforming vart valgt på grunn av mengda informasjon som vart gitt i forhold til ei lita mengde eksperiment. Målet var å sjå påverknaden til elektrisk straum og konsentrasjonen av etansyre på ulike prosessindikatorar. Blant dei var temperatur, pH, coulombisk effektivitet, utbytte, etanats overførselsrate og overførselstid. For å kunne analysere ytelsen vart ulike online-målingar brukt, blant desse pH, temperatur og elektrisk spenning og straum. Prøver frå eksperimentet vart analysert ved hjelp av HPLC. Variansanalyse vart utført på desse resultata for å sjå etter samanhengar og oppdage korleis systemet utvikla seg over tid.

Variansanalysa viste at dei eksperimentelle variablane hadde ein signifikant effekt på den coulombiske effekten og etanats overførselsrate. Interaksjonen var signifikant for dei begge. Resultatet frå variansanalysa viste at det beste operasjonsforholdet var ved høge konsentrasjonar og sterk straum. Den elektriske motstanden viste seg for ein periode på fire timar å vere lågast i det same området, dette indikerar at den optimale økonomiske ytelsen vil i tillegg befinne seg der. Utbyttet viste ingen signifikans. Katalytt-pHen økte i alle forsøka og nådde stasjonær tilstand rundt pH 12.5, medan anodens pH forblei konstant. Temperaturen i begge kammer økte grunna den elektriske motstanden.

Contents

List of Figures

List of Tables

Nomenclature

Symbol	Description	Units	Reference
η	Current effiency	$-$	(Tongwen and Weihua, 2002)
C_0	Equivalent concentration at time 0	$mole/m^3$	(Tongwen and Weihua, 2002)
C	Equivalent concentration at time t	$mole/m^3$	(Tongwen and Weihua, 2002)
V	Circulated volume in each compartment	m^3/s	(Tongwen and Weihua, 2002)
F	Faraday constant	$C/mole$	(Tongwen and Weihua, 2002)
N	Number of cell triplets	$-$	(Tongwen and Weihua, 2002)
I	Current	A	(Tongwen and Weihua, 2002)
t	Time	s	(Tongwen and Weihua, 2002)
E_p	Photon energy	J	(Cornel et al., 2012)
h	Planck constant	Js	(Cornel et al., 2012)
v	Frequency	s^{-1}	(Cornel et al., 2012)
U	Internal energy	J	(Alberty, 2002)
T	Temperature	K	(Alberty, 2002)
S	Entropy	J/K	(Alberty, 2002)
P	Pressure	bar	(Alberty, 2002)
V	Volume	m^3	(Alberty, 2002)
μ_i	Chemical potential of species i	$J/mole$	(Alberty, 2002)
n_i	Amount of species i	$mole$	(Alberty, 2002)
X	Extensive variable	[1]	(Alberty, 2002)
Y	Intensive conjugate variable	[1]	(Alberty, 2002)
μ_i^0	Standard chemical potential of species i	$J/mole$	(Alberty, 2002)
R	Gas constant	$J/moleK$	(Alberty, 2002)
a_i	Activity of species i	$-$	(Alberty, 2002)
z_i	Number of protonic charges on ion i	$-$	(Alberty, 2002)

[1] Dimension varies

F	Faraday constant	$C/mole$	(Alberty, 2002)
Φ_i	Electrical potential of the phase containing species i	V	(Alberty, 2002)
C_i	Concentration of ion	$mole/m^3$	(Tan and Ryan, 2016)
μ_i	Migration mobility	m/Vs	(Tan and Ryan, 2016)
Φ	Electrical potential	V	(Tan and Ryan, 2016)
D_i	Diffusion coefficient	m^2/s	(Tan and Ryan, 2016)
i_{lim}	Limiting current density	A/m^2	(Długołęcki et al., 2010)
F	Faraday constant	$C/mole$	(Długołęcki et al., 2010)
C^b	Bulk solution concentration	$mole/L$	(Długołęcki et al., 2010)
D	Salt diffusion coefficient	m^2/s	(Długołęcki et al., 2010)
δ	Boundary layer thickness	m	(Długołęcki et al., 2010)
t^m_{cou}	Counter ion transport in the membrane	$-$	(Długołęcki et al., 2010)
t^s_{cou}	Counter ion transport in bulk	$-$	(Długołęcki et al., 2010)
$\bar{Y}$	Mean dependent variable		(Rutherford, 2001)
Y_i	Dependt variable at condition i		(Rutherford, 2001)
N	Number of samples		(Rutherford, 2001)
σ	Variance		(Rutherford, 2001)
s	Sample variance		(Rutherford, 2001)
SS_{tot}	Total sum of squares		(Rutherford, 2001)
$SS_{exp.CondX}$	Sum of squares for experimental condition X		(Rutherford, 2001)

Abbreviations and acronyms

ABE Acetone-butanol-ethanol

Anova Analysis of variance

GLM General linear model

HPLC High precision liquid chromotography

IR Infrared

rpm Rotations per minute

SS Sum of squares

SSE Sum of squared errors

1 Introduction

EcoLodge is a research project sponsored in cooporation between Norway and India. Its main goal is an effective production of butyl butyrate from sugars provided mainly from lignocellulose sources. The butyl butyrate ester can be used as a substitute for fossil fuels in diesel engines and jet engines. Butyl butyrate can be used in the chemical industry as a basic building block.

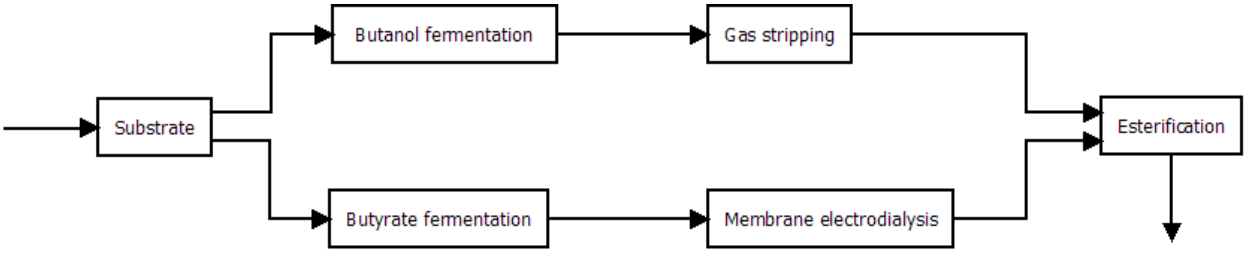

Figure 1: Proposed flowsheet for the EcoLodge setup for production of butyl butyrate.

The fermentation process is divided into two separate reactions, one where the production of butanol is the goal and in the other the fermentation of butyric acid. The proposed setup is shown in fig. 1. In the former gas stripping was used to remove butanol from the fermentation broth and a modelling effort was made by (Birgen et al., 2016). A limiting factor in the model was the concentration inhibition, causing the bacteria to be poisoned. This inhibiting concentration was quite low and caused an increased cost for the separation. The inhibition is present in the butyrate fermentation as well.

The butanol fermentation has several byproducts mainly ethanol and acetone and is also known as ABE fermentation (Maddox, 1989). The ratios between these products could be influenced by different nutrients. For the butyrate fermentation, similar ratios were reported between butyrate, acetate and lactate (Du et al., 2012). Caproate has been reported as another fermentation byproduct (Andersen et al., 2014). A more selective separation could favour the production of the most valuable products. The use of resins could favour certain species (Du et al., 2012) and the pH had an effect on inorganic compounds such as borates (Dydo and Turek, 2013).

For both fermentation reactions the separation is one of the limiting factors as the low concentrations make it less cost efficient and the fermentation culture should ideally not be damaged by the separation. The proposed separation technique for the butyrate was membrane electrolysis. By using an applied current, the anions would be transported across an anion exchange membrane in the direction of the electric field.

Previous experiments have achieved a separation of 96 % in batches (Andersen et al., 2014) and a concentration increase in continuous systems. At low concentrations, the current efficiency remained low with increasing current densities. When concentrating citric acid the use of bipolar membranes was proposed (Tongwen and Weihua, 2002). The experiments showed that the current effiency and power consumption could be altered by the design of the setup. One of the main advantages was the bipolar's production of protons. These were to be supplied to the acid base pair. An increase in selectivity was achieved by the use of charged resins (Du et al., 2012) this favoured the butyrate since it was the largest molecule. The use of resins reduced the current effiency.

In this project experiments on the ion exchange membrane were performed, a factorial design was used to compare multiple variables simultaneously. According to the literature review on membrane electrolysis, this is the first experiment with online measurements. The online measurements included temperature measurement for the cathode and anode, pH measurements for both cathode and anode and Raman spectroscopy. Raman spectroscopy and HPLC was used to measure the composition of the liquid after leaving the anode side. The change in the electrical potential had to be measured by hand during the experiments.

2 Theory

To compare the different experimental results the response used in the statistical analysis was the columbic efficiency. To find this response Raman spectroscopy and HPLC was used to quantify the concentrations.

2.1 Membrane diaelectrolysis

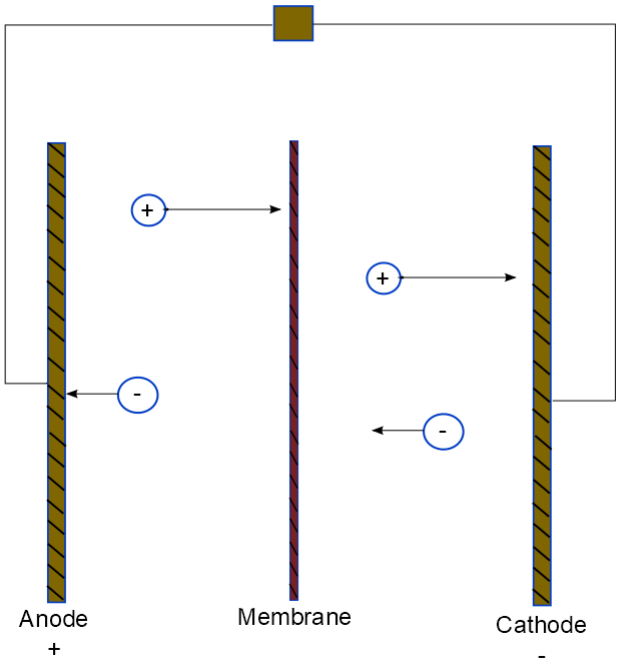

Figure 2: Direction of ion movement by electrodialysis.

Across an ion exchange membrane the ions will strive to reduce the electrochemical potential. This difference creates a gradient across the membrane, fig. (2). The membrane works as a barrier for some of the species based on charge, size or mobility. This creates an uneven distribution of charge, the equilibrium is known as the Donnan equilibrium ((Stell and Joslin, 1986)).

The diluate is the solution from which the specie is removed whilst the concentrate is where it is accumulated.

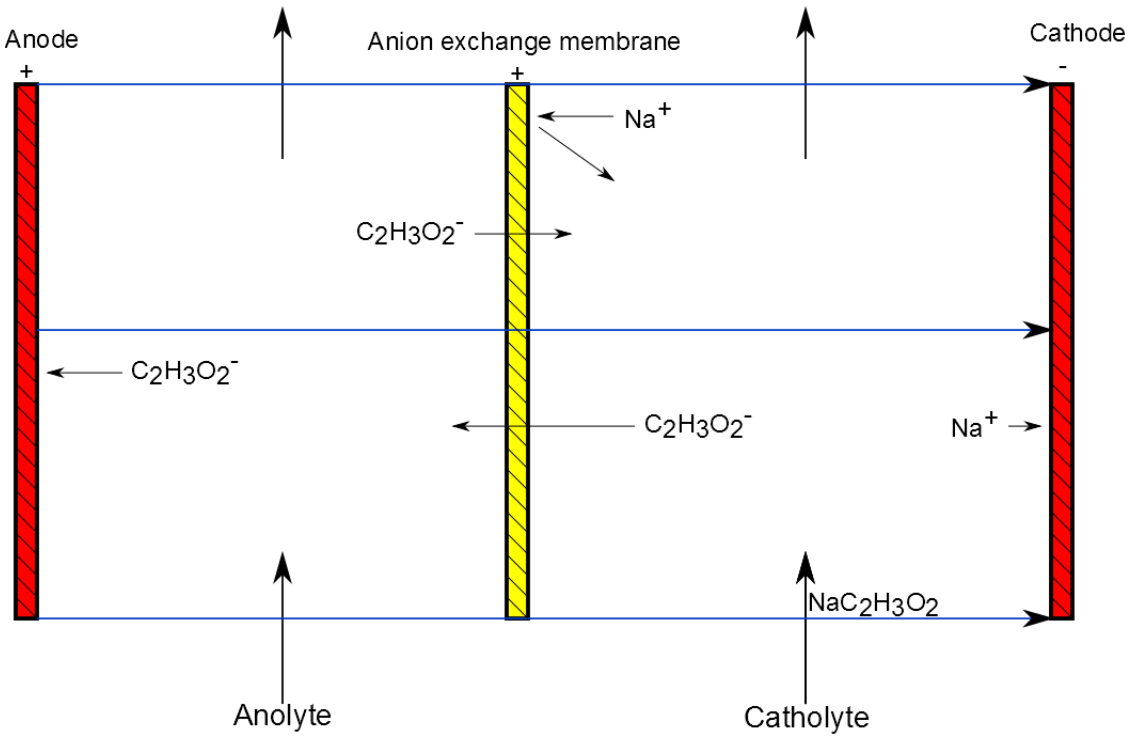

Figure 3: Transport of acetate ions across an anion exchange membrane, the anolyte and catholyte compartments with their respective electrodes. The blue lines indicate the electrical field between the electrodes.

The carboxylic acids will exist in their ionic form to a varying degree depending on the pH of the system. At a higher pH more of the acids will protolyze and be transported more easily across the membrane, the pH can be a technique to regulate the removal in one of the compartments (Andersen et al., 2014).

The acids will be pushed across the membrane by a difference in chemical potential as the driving force, fig. (3). The electrical potential is an addition to the purely chemical potential and by expanding the inner energy and gibbs energy function to include electrical work (Alberty, 2002). This expanded

term can be seen in eq. (1) and (2). U is the inner energy, T the temperature, S the entropy, p the pressure, V the volume, μ the chemical potential and n the number of moles. X and Y is a conjugate pair and could correspond to the electric potential field and the charge.

$$dU = TdS - pdV + \sum \mu_i dn_i + XdY \tag{1}$$

$$\mu_i = \mu_i^0 + RTln(a_i) + z_i F\Phi_i \tag{2}$$

The mass balance for the system can be described by the Nernst-Planck eq. (3) (Tan and Ryan, 2016). This is applicable to the membrane and the entire system. At low potential differences the membrane will have no velocity perpendicular to it and will only be dependent on potential difference. In the overlimiting region of the current voltage curve convection can be observed in the boundary layer (Długołęcki et al., 2010).

$$\frac{DC_i}{Dt} = \mu_i \vec{\nabla}(C_i \vec{\nabla}\Phi) + D_i \nabla^2 C_i \tag{3}$$

2.1.1 Current voltage curve

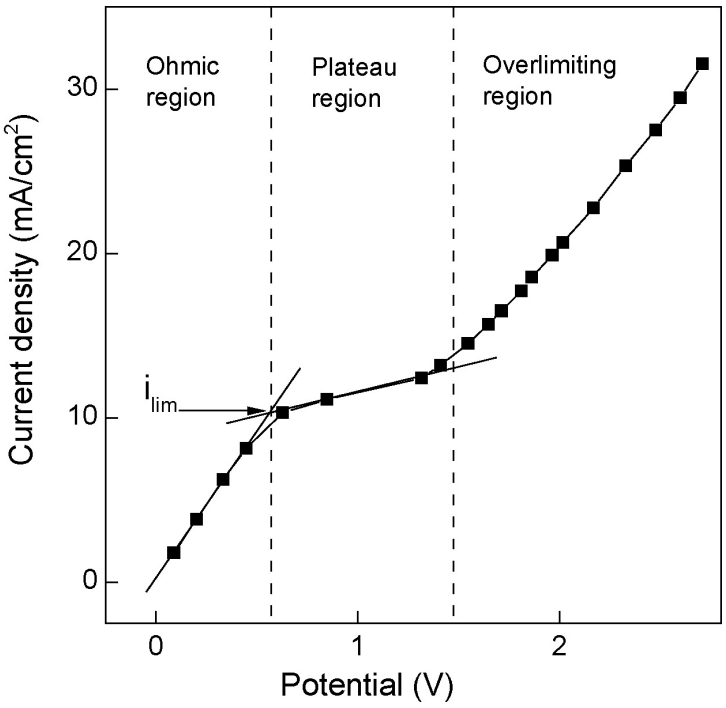

Figure 4: A current voltage curve showing how the current changes with the drop in electrical potential across the membrane ((Długołęcki et al., 2010)).

The current voltage curve illustrates the relation between the current density and the potential drop across the membrane. It is separated into three distinct regions, the ohmic, the plateau and overlimiting region ((Długołęcki et al., 2010)). In the ohmic region there is a linear relationship between the drop in potential and the current density and continues until it reaches the limiting current density. An expression for the limiting current density can be found in eq. (4). Here i_{lim} is limiting current density, F the Faraday constant, C^b the bulk solution concentration, D the diffusion coefficient, δ the boundary layer thickness and t^m_{cou} and t^s_{cou} the transport numbers in the membrane and the bulk.

$$i_{lim} = \frac{FC^bD}{\delta(t^m_{cou} - t^s_{cou})} \tag{4}$$

In the plateau region the current density has a lower increase compared to the other regions. In this region the solutes are less likely to accumulate in the boundary layer. In the overlimiting region the current density will increase further. In the two latter regions electro-convection will occur in the boundary layer ((Rubinstein and Zaltzman, 2000)). When the current limiting density is reached a reduction in the solute concentration close to the membrane surface can be observed ((Tanaka, 2012)).

At the limiting current density water dissociation, eq. (5), can occur on the active groups on the membrane. This will in turn have an effect on the pH of the diluate solution (Strathmann, 2004b).

$$\mathrm{H_2O} = \mathrm{H^+} + \mathrm{OH^-} \tag{5}$$

2.1.2 Reactions on the electrodes

If the electrical potential over the membrane is higher than 1.23 V hydrogen and oxygen will be produced. Hydrogen will be reduced on the cathode according to eq. (6) whilst oxygen is oxidized on the anode. The biproducts from the reactions namely hydroxide ions and protons are separated by the membrane and are free to react with other species in the solution. The protons on the anode can react with the organic acids and through a high concentration at equilibrium stop the acid from being in ionic form.

$$2\,\mathrm{e^-} + 2\,\mathrm{H_2O} = 2\,\mathrm{OH^-} + \mathrm{H_2} \tag{6}$$

$$\mathrm{H_2O} = 2\,\mathrm{H^+} + \mathrm{O_2} + 2\,\mathrm{e^-} \tag{7}$$

$$\tag{8}$$

2.2 Coulombic efficiency

The Coulombic efficiency compares the amount of charge transported across the membrane for one or more species. A high Coulombic efficiency implies that the electric charge is mainly used to transport the ions. Its calculation is given in eq. 9, (Tongwen and Weihua, 2002). The concentrations C are for the diluate side at time zero and at a measured time. V is the volume of diluate compartment, in this project that corresponds to 500 mL. N is

the number of cell pairs and is defined the following way: "A unit composed of a cation exchange membrane, a compartment with the dilute, an anion exchange membrane and the concentrate department is referred to as a cell pair" (Strathmann, 2004b). In this case this would correspond to 1.

$$\eta = \frac{(C_0 - C_t)VF}{NIt} \tag{9}$$

2.3 Raman spectroscopy

The two most common types of vibration spectroscopy are the IR spectroscopy and the Raman spectroscopy. The IR spectroscopy is also known as Rayleigh scattering. The Rayleigh scattering process is an elastic process whereby the energy delivered by a photon to heighten the vibrational state of the molecule will be returned when the molecule returns to its natural state (Cornel et al., 2012). The energy of the photon will be directly related to the frequency, eq. (10), where E_p is the energy of the photon, h is Planck's constant and v the frequency.

$$E_p = hv \tag{10}$$

At a given temperature most of the molecules will be in a certain vibrational state, but there will be molecules in other states as well. When a molecule is hit by a photon it can be excited from that state to the excited state or excited from its natural state. The emitted photon can have a lower or higher energy than the incoming photon. This difference in absorption and emission energy is characterized as an inelastic process.

The probability of a photon energy lower than the absorption energy is higher than the probability of a photon with higher energy. At room temperature most of the molecules will be in the ground state, this increases the probability of lower energy emitted photons (Larkin, 2011). The lower energy photons are known as the Stokes Raman scattering and the high energy as the anti-Stokes Raman scattering.

The Raman scattering intensity is significantly lower than that of Rayleigh scattering and will require efficient detectors. The density of the sample is

important to get a sufficiently large amount of signals, therefore Raman spectroscopy is mainly applicable to solids and liquids. Both the solute and the solvent will influence the spectrum. Water has a small impact as a solvent (Cornel et al., 2012).

Near infrared signals have less defined peaks than the Raman spectroscopy. This reduces the need for more advanced methods for analysis (Frauendorfer and Hergeth, 2017). The probes and the spectrometer are connected through optical fibres. These can be easily damaged by contact or removal. When running the experiments a single frequency laser is used, usually in the near infrared area 750-1400 nm, thereby making them monochromatic.

2.4 Factorial design

In factorial design a fixed number of levels for each variable can be chosen. The levels can be quantitative or qualitative, the quantitative can be a given concentration or electrical current. An experiment will be performed for each combination of variables. The number of runs is the product of the levels.

A common approach is the two level factorial approach, which with a few runs can explore major trends and propose further investigation, tab. (1). From these observations the effects of the variables and the interactions can be investigated. A common way to display the design is through a design matrix (Box et al., 1978).

Table 1: Example of design matrix for a 2^3 factorial design. A, B and C are variables and + and - represent the max and min of the levels. The last column is the effect.

Run	A	B	C	
1	-	-	-	1
2	+	-	-	a
3	-	+	-	b
4	+	+	-	ab
5	-	-	+	c
6	+	-	+	ac
7	-	+	+	bc
8	+	+	+	abc

If 3 levels are used the levels are divided into the following levels, -, 0 and +, tab. (2).

Table 2: Example of design matrix for a 3^2 factorial design. A and are variables and +, 0 and - represent the max, middle and min of the levels.

Run	A	B
1	-	-
2	0	-
3	+	-
4	-	0
5	0	0
6	+	0
7	-	+
8	0	+
9	+	+

The effect is the change in yield if it is moved from the + level to the - level, when the other factors remain constant. The main effect will be the average of all effects for that variable for all conditions. The two-factor interaction will be half the difference between the average effect for the first variable at the + and - for the second variable. The three faction interaction is the difference of the two factor interaction when the third variable is kept constant divided by two. When there is a large interaction the variables cannot be considered separately.

To achieve an estimate for the variance, replicates of the experiment have to be done. Otherwise it has to be assumed that the higher-order interactions are negligible. This is because the number of degrees of freedom is too low. This can be justified by that main effects and lower-order interactions are usually larger.

2.4.1 Yate's algorithm

The Yate's algorithm describes a way to set the observations in standard order. The first column consists of successive - and + signs, the second column of successive pairs of - and +. The last column will be made up of 2^{k-1} - signs

followed by the equal number of + signs. The system is analogous for a three level design.

2.5 Analysis of variance

Analysis of variance or ANOVA can be considered as model plus an error (Rutherford, 2001). The outcome will be the dependent variable and the experimental conditions the experimental variables. Compared to the t-test the error type 1 does not increase with more significance tests. The test used in ANOVA is F-test and is calculated with help from the variance. The variance can be found through the mean, eq. (11), and is shown in eq. (12). To get am unbiased estimate the sample variance is often used instead eq. (13).

$$\bar{Y} = \frac{\sum_{i=1}^{N} Y_i}{N} \tag{11}$$

$$\sigma^2 = \frac{\sum_{i=1}^{N} (Y_i - \bar{Y})^2}{N} \tag{12}$$

$$s^2 = \frac{\sum_{i=1}^{N} (Y_i - \bar{Y})^2}{N - 1} \tag{13}$$

The total sum of squares tells the difference from the total mean value and the observations, eq. (14). The sum of squares can be found within the different experimental conditions, eq. (16), as well and the sum of squares between the groups. Between the groups it is the group mean subtracted by the overall mean, eq. (17). The total sum of squares is related to the within sum of squares and the between sum of squares by eq. (18).

$$SS_{tot} = \sum_{i=1}^{N} (Y_i - \bar{Y})^2 \tag{14}$$

$$SS_{exp.condX} = \sum_{i=1}^{N} Y_i^2 - (\sum_{i=1}^{N} Y)^2 \tag{15}$$

$$SS_{within} = \sum_{X=1}^{M} SS_{exp.condX} \tag{16}$$

$$SS_{between} = \sum_{j=1}^{p} N_j (\bar{Y}_j - \bar{Y}_G)^2 \tag{17}$$

$$SS_{tot} = SS_{between} + SS_{within} \tag{18}$$

The degrees of freedom for the variables and the conditions are N-1. The mean square can be calculated as the square divided by the degrees of freedom. To test for significance the F-test is used where the mean of squares within the treatment divided by mean square between treatments are tested against tabulated F-values.

2.5.1 Analysis of variance for factorial designs

In eq. (19) the model of a two variable factorial design is shown. The equation has the interaction term between the two variables to add that effect. The mean is calculated from all the experimental conditions, whilst the main effect effects are the difference on that condition from the mean eq. (20), the mean μ_j is defined in eq. (21). p and q are the number of levels for each variable. The interaction effect at a given condition is given by eq. Any interactive effects at a point are found through eq. (22).

$$Y_{ijk} = \mu\alpha_j + \beta_k + (\alpha\beta)_{jk}\epsilon_{ijk} \tag{19}$$

$$\alpha_j = \mu_j - \mu \tag{20}$$

$$\mu_j = \sum_{k=1}^{q} u_{jk}/q \tag{21}$$

$$(\alpha\beta)_{jk} = \mu_{jk} - (\mu + \alpha_0 + \beta_o) \tag{22}$$

The null hypothesis will assume that the tested factor does not influence the data. This can be applied to the model and when one of the factors is

zero it is called a reduced GLM (Rutherford, 2001), eq. (23). To calculate the error sum of squares eq. (24) is applied, in the equation the term $\hat{Y}_{ijk}$ changes depending if it is a reduced GLM or a full GLM. For full GLM $\hat{Y}_{ijk} = \bar{Y}_{jk}$, whilst for the reduced GLM $\hat{Y}_{ijk} = \bar{Y}_{jk} - \alpha_i$. The α is estimated in eq. (25) as the difference between the marginal and grand mean. By substituting it into eq. (24) eq. (26) can be obtained, N_{jk} is the number of subjects in an experimental condition. A similar equation can be developed for the interaction effect, eq. (27).

$$Y_{ijk} = \mu + \beta_k + (\alpha\beta)_{jk}\epsilon_{ijk} \tag{23}$$

$$SSE = \sum_{k=1}^{q}\sum_{j=1}^{p}\sum_{i=1}^{N}(Y_{ijk} - \hat{Y}_{ijk})^2 \tag{24}$$

$$\hat{\alpha} = \bar{Y}_i - \bar{Y}_G \tag{25}$$

$$SSE_{ARGLM} = SSE_{FGLM} + N_{jk}q\sum_{j=1}^{p}(\bar{Y}_j - \bar{Y}_G)^2 \tag{26}$$

$$SSE_{ABRGLM} - SSE_{FGLM} = N_{jk}\sum_{k=1}^{q}\sum_{j=1}^{p}(\bar{Y}_{jk} - \bar{Y}_j - \bar{Y}_k + \bar{Y}_G) \tag{27}$$

Given the degrees of freedom the mean squares can be calculated, thereby giving the F-values.

3 Materials and methods

3.1 Experimental setup

3.1.1 Membrane specifics

Table 3: The dimensions and descriptions of the membrane parts. The data was given by K. Verbeeck and P. Candry (Personnal communication. Email 16.01.2017).

Layer	Length [cm]	Width [cm]	Thickness [cm]	Other features	Description
Anode outer case	28	13	2	8 bolt holes to stabilize the membrane and a hole in the middle to let the anode through.	Outer case to stabilize the membrane.
Anode inner case	24	9	2	Inner frame for the liquid of 20x5x2cm	Flow compartment for the anode side.
Anode	20	5	0.1	Coarse lattice connected to the power supply through the outer case by a metal tube of 5 cm	Ir MMO coated titanium electrode with a centrally attached, perpendicular current collector.
Rubber layer	24	9	<0.1	Inner frame of 20x5x0.1cm	Rubber between the layers will hinder leakages of gas and liquid.

Spacer	20	5	<0.1	Lattice formed surface approximately the size of the anode lattice	Preventing contact between membrane and electrodes.
Membrane	23	8.5	<0.1	-	Fumasep anion exchange membrane
Cathode	20	5	0.1	Has a connection to the current outlet through the inner case 2x2 cm.	Stainless steel wire mesh.
Cathode inner case	24	9	2	Inner frame for the liquid of 20x5x2cm. Has an additional opening on the side for the power connection.	Flow compartment for the cathode side.
Cathode outer case	28	13	2	8 bolt holes to stabilize the membrane.	Outer case to stabilize the membrane.

Tab. 3 shows the dimensions and other distinctiveness of the membrane layers. The anode outer case stabilized alongside with cathode outer case the membrane structure. There were 8 bolt holes connecting it with the outer cathode case on the sides. Placed in the middle was a separate opening for the power supply of the anode, through which the metal tube connecting the anode could be placed. The outer case was connected to the wooden frame of the experimental setup by two bolts running from the bottom of the case.

The anode inner case was the liquid body for the anolyte and had a volume of 200 mL. The anode would be placed within this volume and the spacer material. The inlet and outlet would on the opposite sides of each other and placed in the middle on both sides.

The anode had a metal tube as a current collector, this was perpendicular to the main anode surface which consisted of a lattice made up of Ir MMo coated titanium. A spacer material was placed between it and the membrane to stop any contact between them from occurring. Its position within the anode inner case could be locked by tightening the connection of the current collector after it had left the outer case.

Rubber layers were placed between each case and between the membrane. Their main purpose was to stop gas and liquid leakages. All the rubber pieces were of the same size. The spacer material was formed as a lattice and its shape was similar to the anode surface. The spacers were placed between the membrane and the electrodes in the liquid compartments of the inner cases.

The cathode was a steel wire mesh that was finer than the anode lattice. Electric current was provided by a connection through the side of the cathode inner case. The membrane was a Fumasep membrane for anion exchange.

The cathode inner case had the same dimensions as the anode inner case and its inlet and outlet points were in the same position. On the side there was another opening for the current connection for the cathode. The cathode outer case was built in a similar manner to the anode outer case except the lack of an opening for the power connection.

In fig. 5 the structure of the membrane can be seen. The difference between the anode and cathode inner case should be noted due to the gas outlet above the cathode.

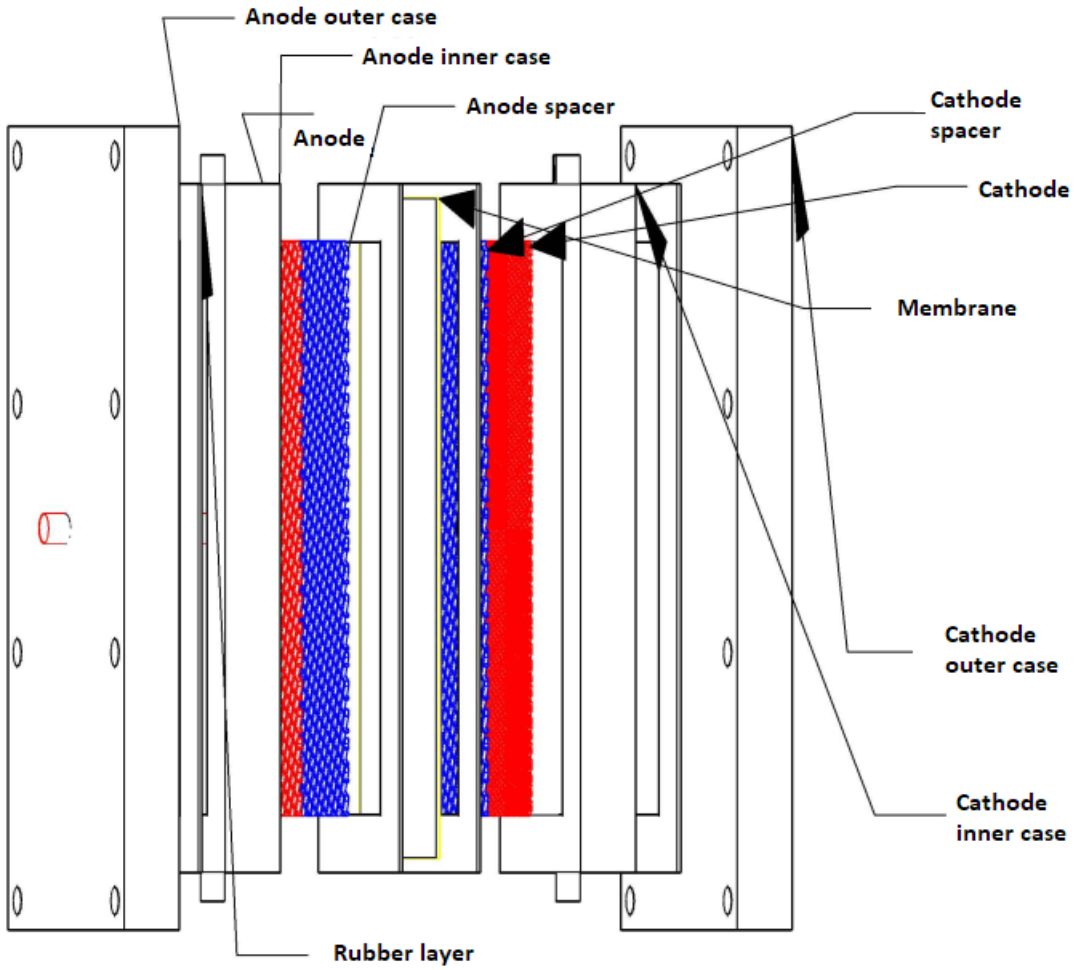

Figure 5: The structural design of the membrane with its supporting inner and outer cases and rubber layers placed between.

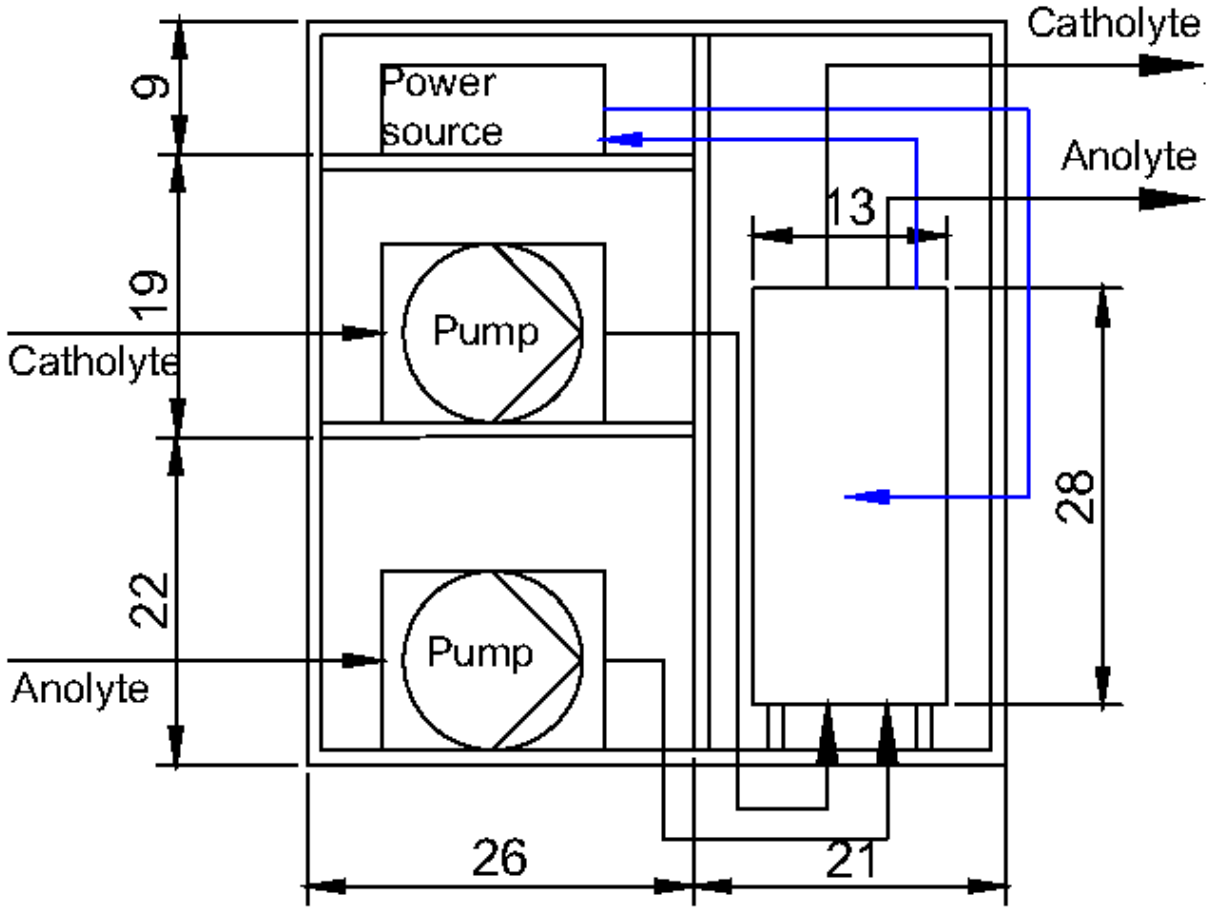

Figure 6: The dimensions of the experimental setup with positions of the pumps and power source. The flow directions are shown. The blue lines are the power connection.

The dimensions of the experimental setup are given in 6. The diluate and the concentrate were co-current and two pumps supplied the samples from the containers. The outlet streams were collected in separate containers from which Raman spectroscopy could be applied to measure the concentrations

of the different components. In fig. 7 the connections of the setup can be seen when it designed co-current.

During the experiments the power source worked with a constant electric current and the voltage varied depending on the resistance. The throughput of the pumps could be adjusted by changing the rotations per minute, changing the flow direction was a possibility as well.

3.1.2 Pumps

The pumps which were used were the Watson Marlow 300 series pump. The flow direction and the rpm-value could be adjusted

3.1.3 Membrane

The membrane was a Fumasep anion exchange membrane.

3.1.4 Electrodes

There were two kinds of electrodes, a stainless steel wire mesh electrode and a 2 Ir MMO coated titanium electrodes with a centrally attached, perpendicular current collector. The Ir electrode was the anode. The membrane was bolted to the setup by two bolts connected to the outer case. Bolts connecting the outer cases kept the membrane supported.

3.1.5 Labview

Labview was used to log all continuous data from the experiments, this included pH, temperature and electrical potential and current. All the signals from the probes were sent to the same computer.

3.1.6 Power supply

The power supply used in the experiment was the TDK-Lambda Z series and supplied direct current. The user manual supplied the information about how to run it with a constant current and measurements of the electrical current and voltage could be done (TDK-Lambda (2012)). The power supply could run in two operating modes in the standard mode, these were constant

current and constant voltage. The maximal acquirable potential was 10.50 V and if the potential exceeded this limit in constant current mode it would at that limit operate at constant potential unless the potential decreased. Other setups would require the programming and monitoring through an USB or other tools. An USB cable was used to connect the power supply with the computer running labview logging the electrical current and potential.

3.1.7 pH

The pH was measured by two Mettler electrodes and logged in labview. Both electrodes were calibrated using a pH 4 and pH 7 solution.

3.1.8 Temperature

Temperature was measured by Mettler thermometer and the data supplied to labview.

3.1.9 Raman spectroscopy

A Raman spectrometer was connencted to the anode outlet and had the following settings:

- Measurement time: 5000 ms
- Averages: 6
- Delay: 50000 ms

And for every new measurement a new dark was taken. The frequency applied was 785 nm.

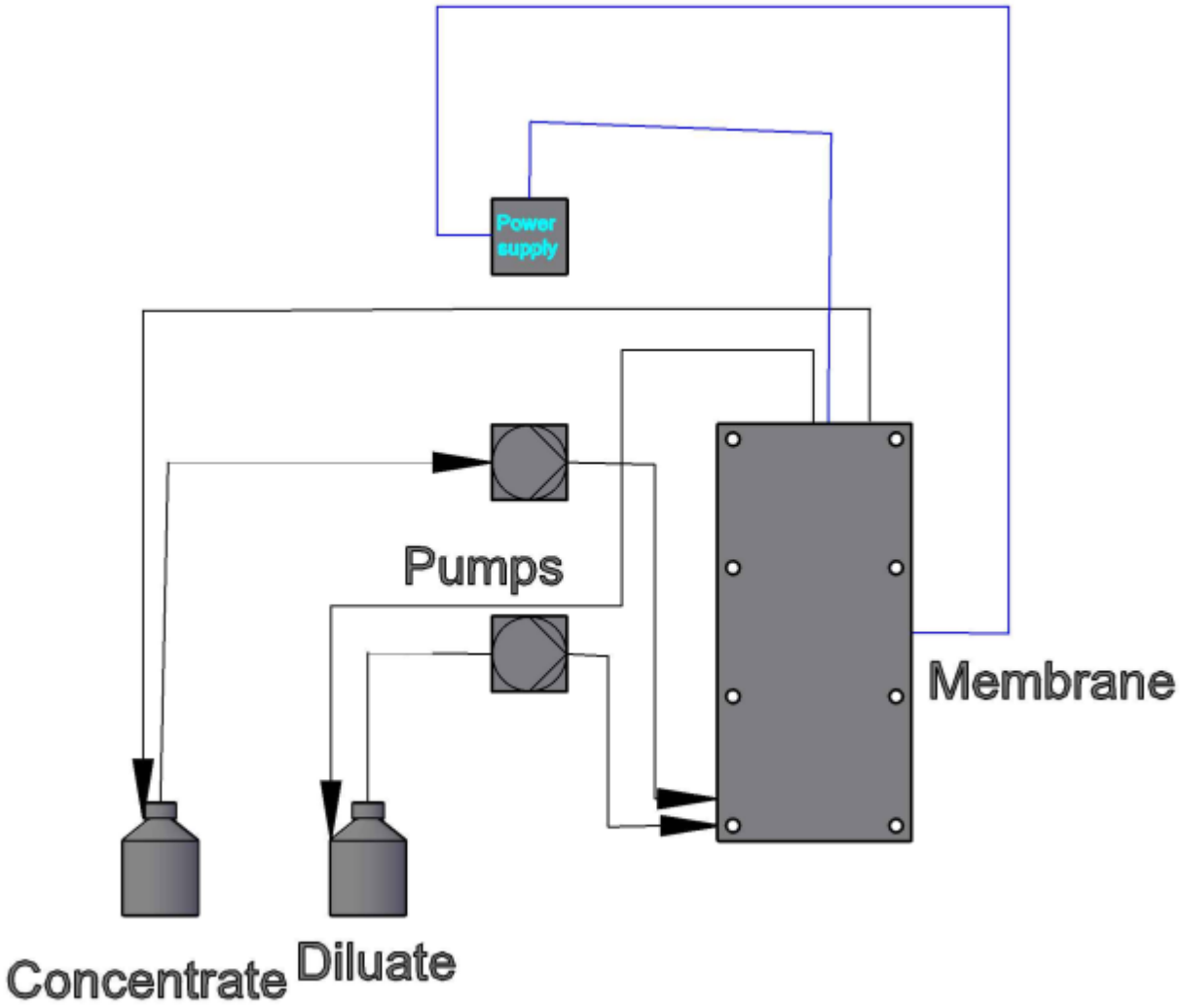

Figure 7: Setup of the membrane drawing in 3D seen from the front, it shows the actual positions of the flow and power connectors and the liquid pathways.

3.2 Materials

100% acetic acid was used as the basis to make the diluted solutions. 1 M NaOH was used to adjust the pH to 8, the set point for the adjustment was 8 (personal communication Kristof Verbeeck, email, 03.04.2017). 1 M H_2SO_4 was used to make the anode solution at pH 2.

3.3 Experimental design

A factorial design was chosen to get an overview of the operating conditions with the fewest number of experimental runs. Tab. (4) shows the different samples and operating conditions for the experimental runs. To reduce the number of variables both pump throughputs would be kept constant at 80 rpm and because leakages were observed at higher pump speeds. A smaller difference in pump throughput would have explored only a small part of what should be possible and therefore would it give less insight to the effect of the pumps. In this part of the experiment acetate was the only specie, used to remove any influence from the other components.

Table 4: The different samples and conditions used for experiments on a membrane with an acetate in water solution using a 3x2 factorial design.

c [%]	I [A]
0.5	0.3
1	0.3
2	0.3
0.5	0.5
1	0.5
2	0.5

3.4 Methods

3.4.1 Experimental procedure

Before each experiment the pH probes were calibrated by using 4 and 7 pH calibration standards. The power supply was given a setpoint on which constant current would apply. Until that point the system would operate with

Table 5: List of experiments in a 2x3 factorial experiment with 1 repetition.

Run	c [%]	I [A]
1	0.5	0.5
2	0.5	0.5
3	1	0.5
4	1	0.5
5	2	0.5
6	2	0.5
7	0.5	0.3
8	0.5	0.3
9	1	0.3
10	1	0.3
11	2	0.3
12	2	0.3

a constant voltage of 10.50 which was the maximum the power supply was capable of. The anode solution was made by mixing H_2SO_4 in water providing the electrolytes in that compartment. Electrolytes were needed in both compartments to stop the development of a too great osmotic pressure difference. A 1 M H_2SO_4 solution was added to the anode compartment in an amount that gave its desired pH. On the cathode compartment acetic acid was added according to the experimental design and 3 M NaOH was used to adjust the pH. The solutions were made in 1 L batches and kept in closed bottles to avoid losses to evaporation.

The pH of the anode was set to 2 and 8 for the cathode. The pH of the cathode would vary to a stronger degree because acetic acid had passed the half equivalence point and was very sensitive to the addition of strong acids and bases. The pH was observed online in both liquid compartments and the composition was measured through a Raman spectrometer at the outlet of the membrane. The change in electrical potential was recorded every hour. when the online measurement of the potential was ready data was recorded through a data logger. Samples from the outlet were taken to be analysed by HPLC. Raman spectroscopy was used to analyse the samples before and after the experiments and were to be compared with the HPLC results. The experimental design had one repetition.

Each experimental run would start with the pumps removing liquid from their separate containers and filling the liquid body of the membrane. The power could then be turned on creating the potential difference across the membrane. The electric current would be controlled and held constant during the experiment. The experiments were performed in a randomized order different from tab. (5).

3.4.2 Analysis of the data

All statistical analysis was performed using the software Minitab 17. The anova had no quadratic terms to save degrees of freedom and since it could available for only one of the two variables. The softwares Matlab and Python were used to treat the large amount of information coming from the data logging. Matlab as a plotting tool for the pH, temperature, concentration and electrical potential and current whilst Python performed the plotting for the Raman data.

3.4.3 Measurements

The pH probes and thermometers were kept in the liquid containers which were the sources of the inlet to the membrane. HPLC was used to find the composition of the solutions at the start and end of experiments. The efficiency was calculated according to eq. (9). The volume was 500 mL.

4 Results

4.1 Experimental data

For all runs with online current and potential logging and its replica ,the average of the two runs was used, fig. (8) to fig. (10). Each run that did not have online current and potential logging the replica had it, these replicas are shown on fig. (11) to (13). All runs without online logging of these parameters are shown in the appendices, fig. (25) to (27).

In the 2x3 factorial experiment there was a clear increase in the temperature in the anolyte and catholyte. This can be seen in fig. (25) to (10). The room temperature was kept constant at 22 °C and the temperature increased beyond it. A test on the thermometers showed that the one on the anolyte measured a temperature approximately 1.6 °C higher than that of the catholyte. In run 4, fig. (12), the temperature of the anode and pH changed after 3 hours due to the pump connection was not fully beneath the liquid level and the transport of liquid through the membrane was reduced. After three hours the problem was detected and dealt with.

For all experimental runs with a concentration of more than 0.5% the electrical potential increased during the experiment. By lower concentrations the opposite occured. Statistical analysis showed that the potential change could be described by linear regression. From fig. (28) to fig. (34), the R-values indicated a good fit to the data. An analysis of variance showed that the regression was significant. The end potential was lower for 2% solutions and higher currents gave a lower electrical resistance after 4 hours compared to the start.

The last plot on each figure is the change in concentration for the anode and cathode compartments, the values were taken from the HPLC data. In the first two plots, fig. (25) and (11) the anode end concentration is higher than the catholyte. Due to the low value of both outlet compartments mass conservation is not fulfilled.

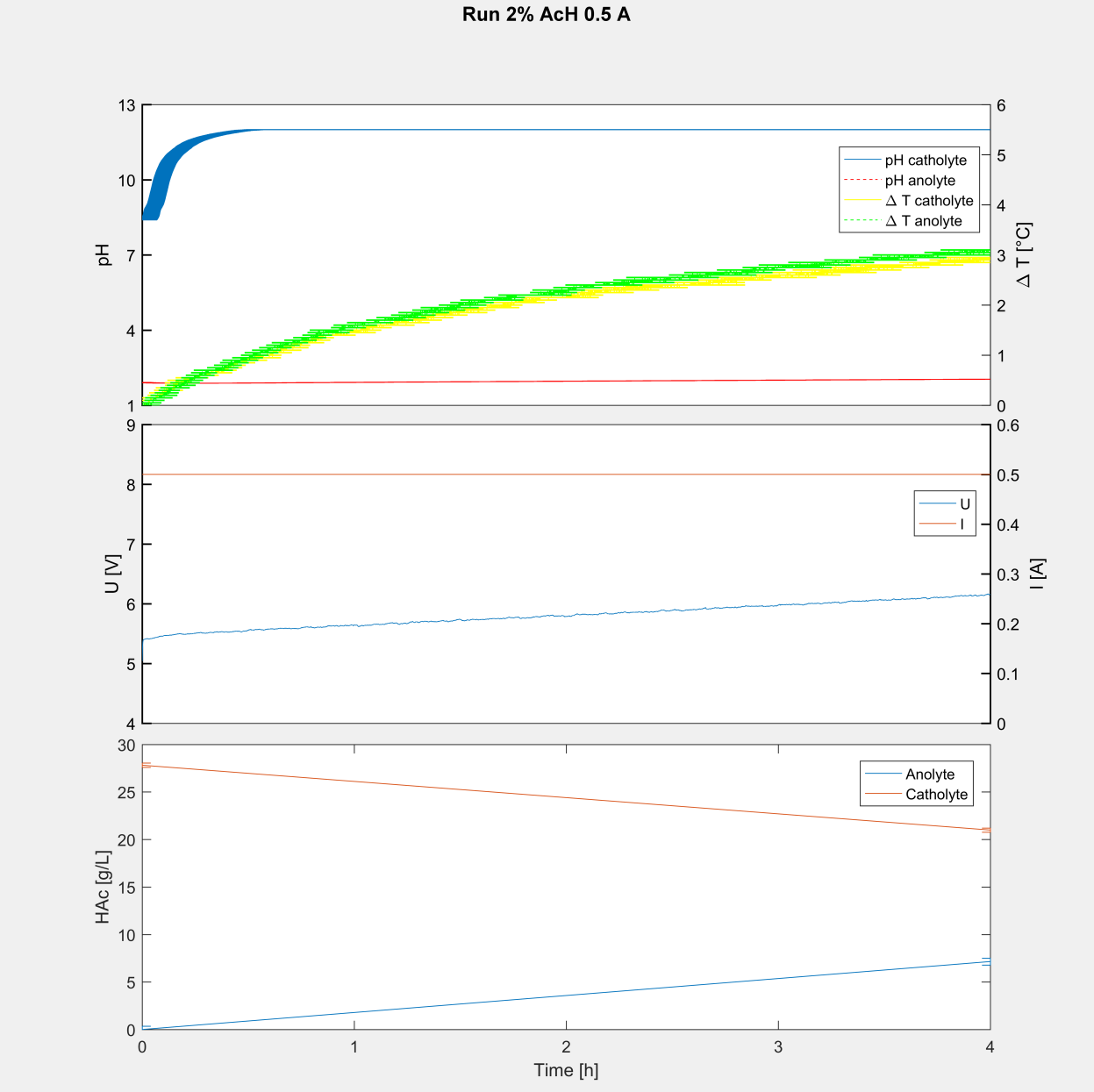

Figure 8: Development of pH, temperature, electrical potential and current and change in concentration for an experimental run using 2% acetate and an electrical current of 0.5 A.

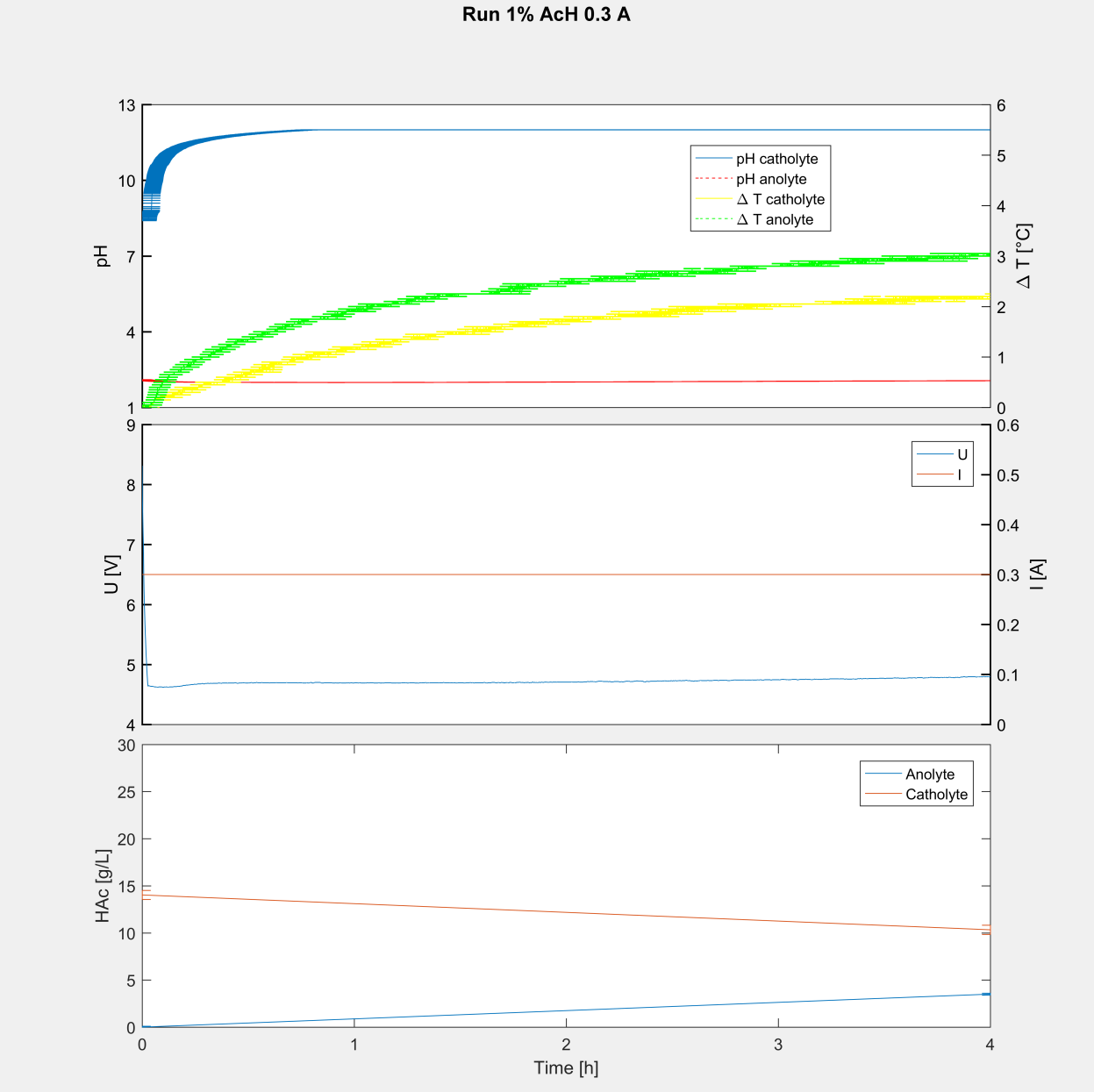

Figure 9: Development of pH, temperature, electrical potential and current and change in concentration for an experimental run using 1% acetate and an electrical current of 0.3 A.

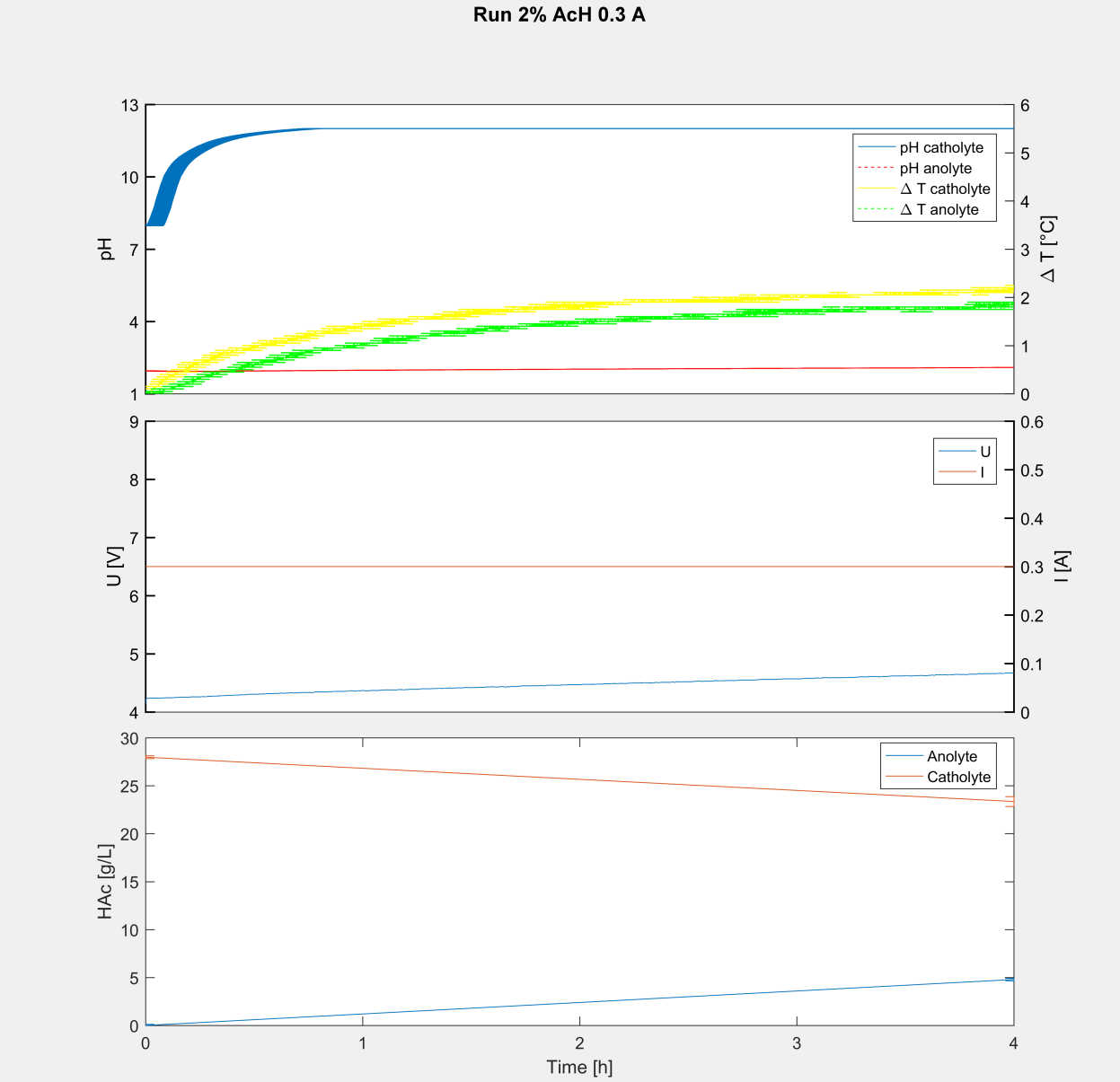

Figure 10: Development of pH, temperature, electrical potential and current and change in concentration for an experimental run using 2% acetate and an electrical current of 0.3 A.

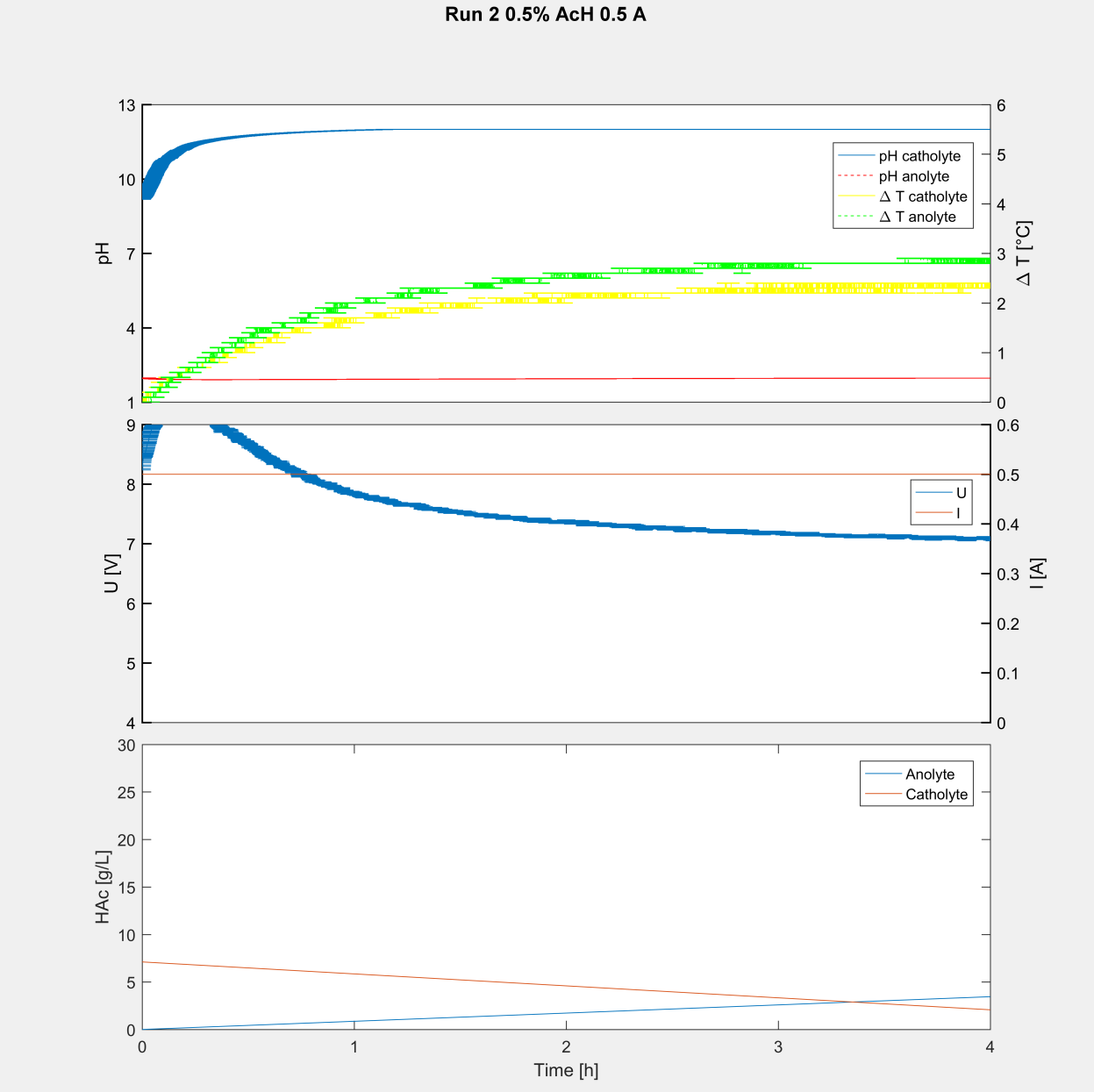

Figure 11: Development of pH, temperature, electrical potential and change in concentration for an experimental run using 0.5% acetate and an electrical current of 0.5 A.

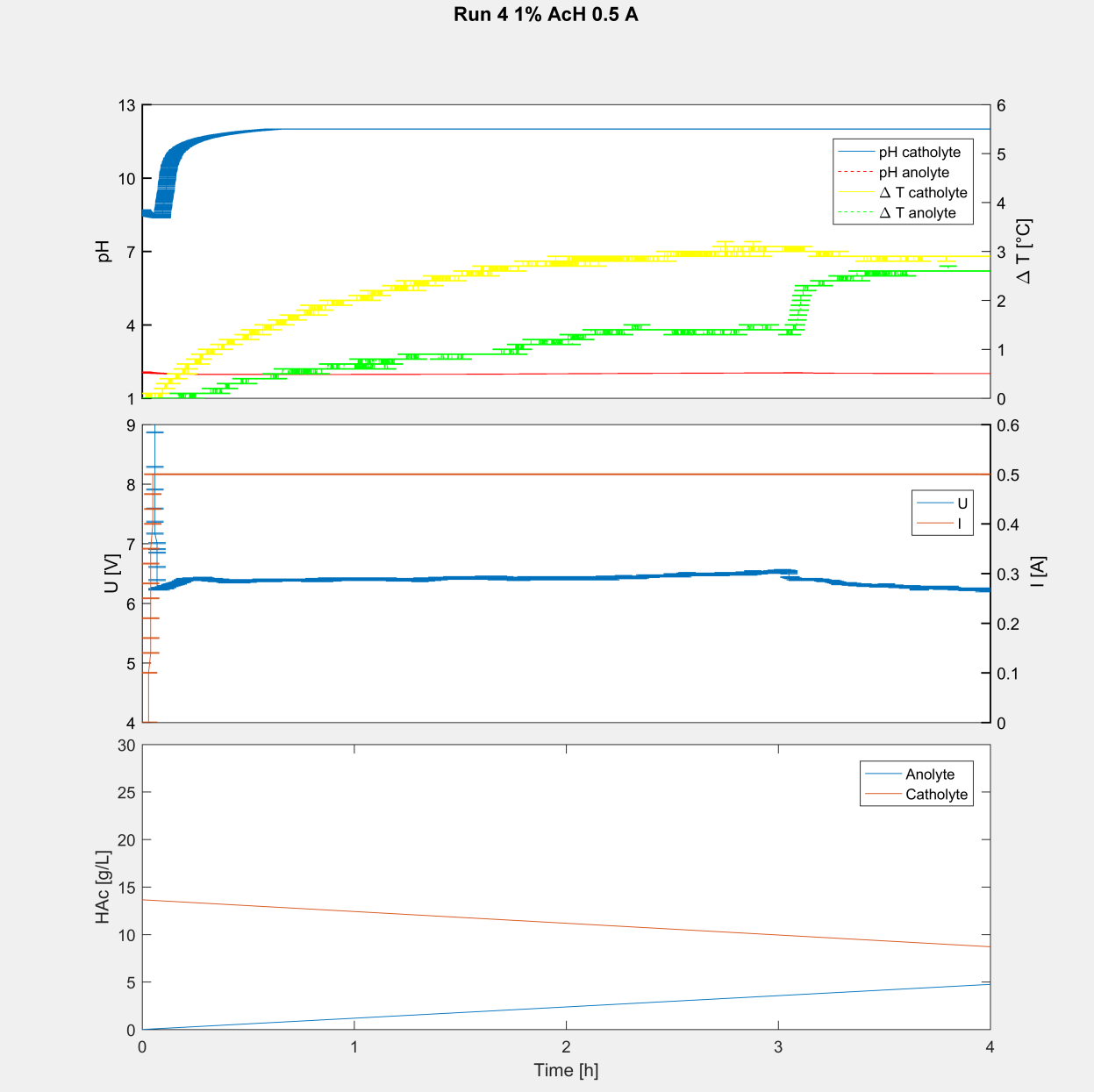

Figure 12: Development of pH, temperature, electrical potential and current and change in concentration for an experimental run using 1% acetate and an electrical current of 0.5 A.

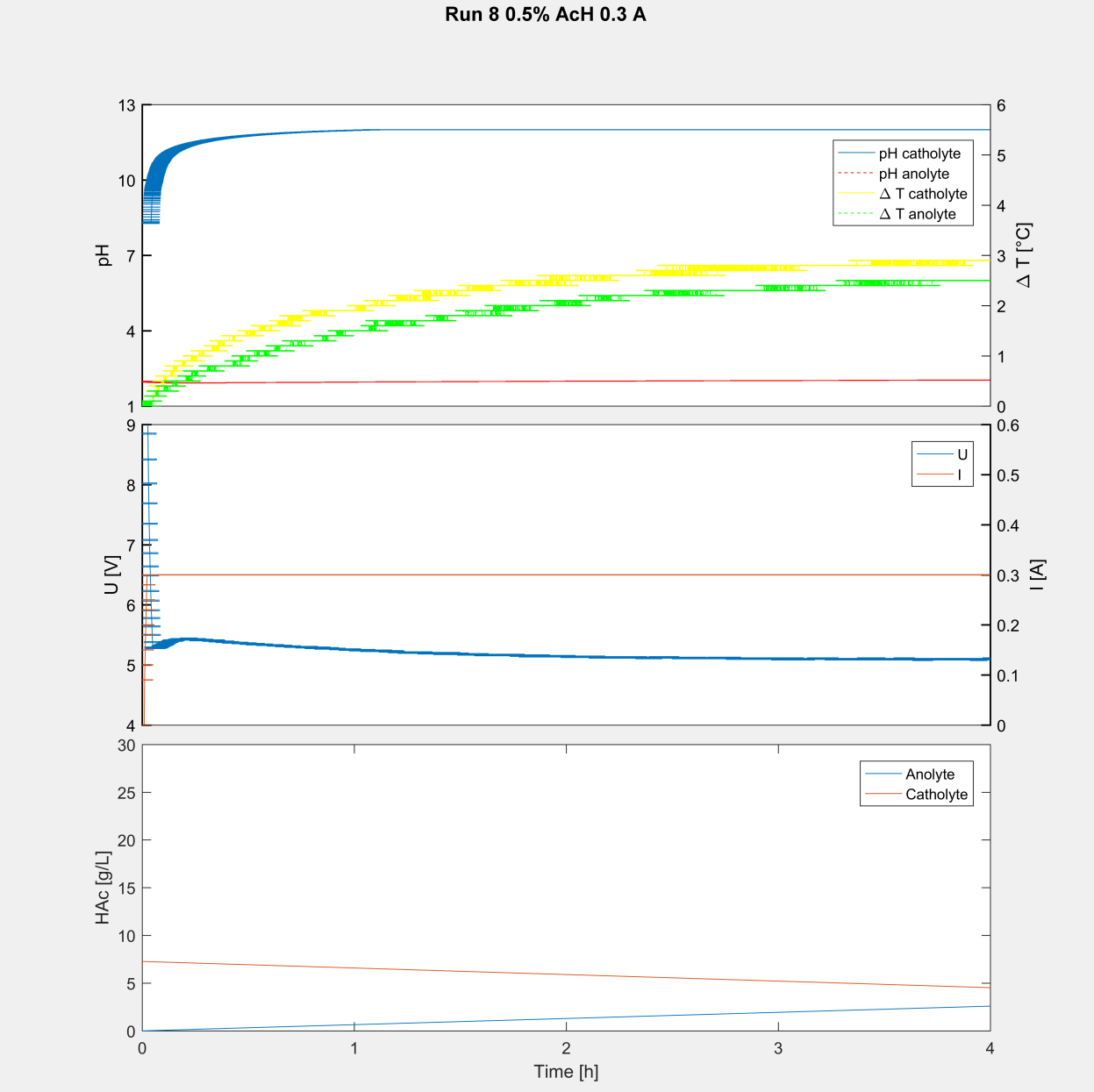

Figure 13: Development of pH, temperature, electrical potential and change in concentration for an experimental run using 0.5% acetate and an electrical current of 0.3 A.

4.2 Discolouration of the anolyte

At all currents a change in colour in the anolyte was observed. No discolouration was observed in the catholyte. The HPLC gave no indication of the substances involved.

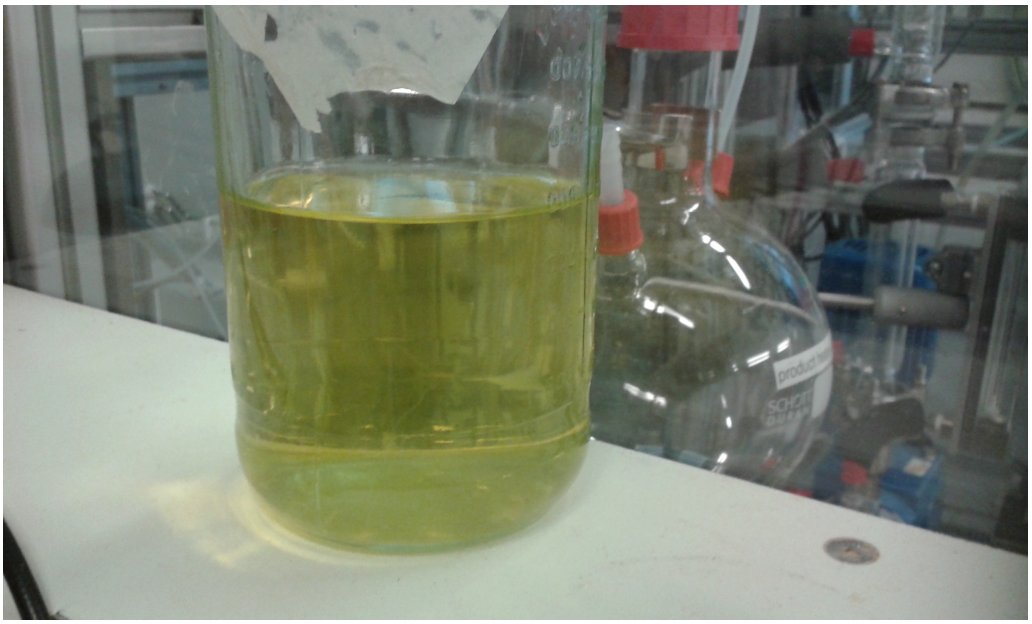

Figure 14: Observed change in colour of the liquid in experiments.

4.3 Raman spectrometry

The Raman spectrometer was able to detect a 5% solution of acetic acid in water (15). The main peak was visible at around 844 nm. At two percent the peak was still detectable, fig. (16), although smaller than the peaks caused by the noise. At one percent the difference between a peak and noise was not discernible to the eye, fig. (17).

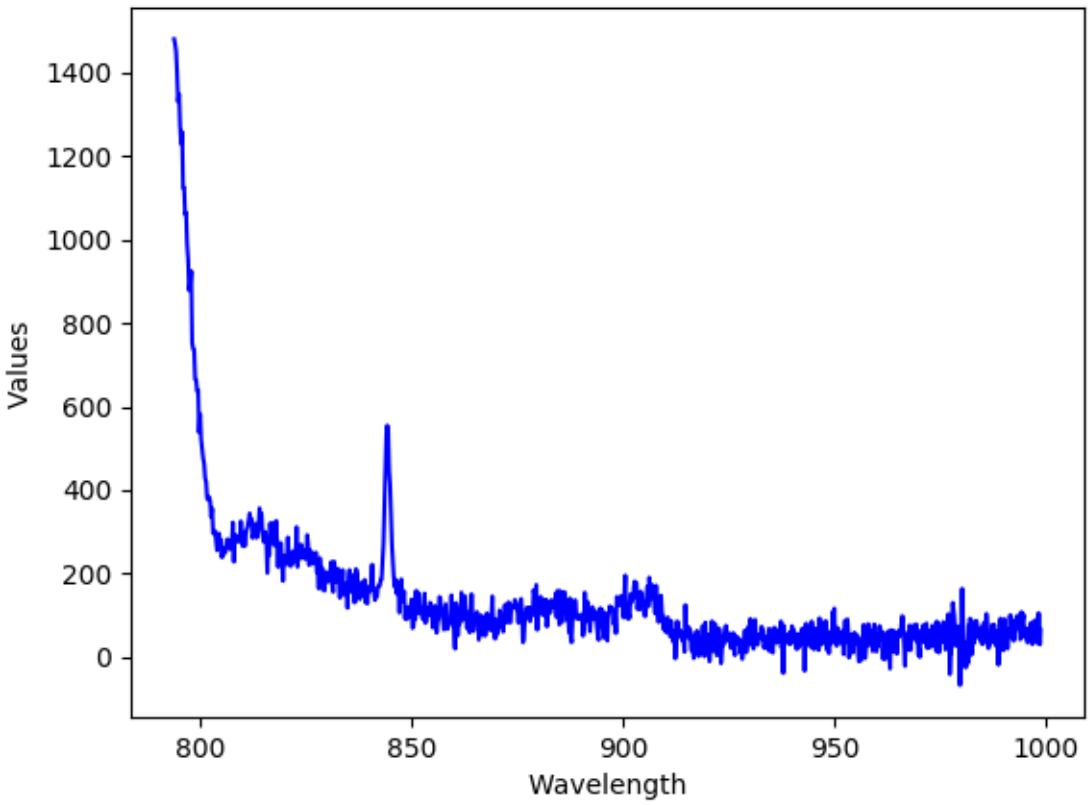

Figure 15: Raman spectra of a 5% HAc standard solution in water.

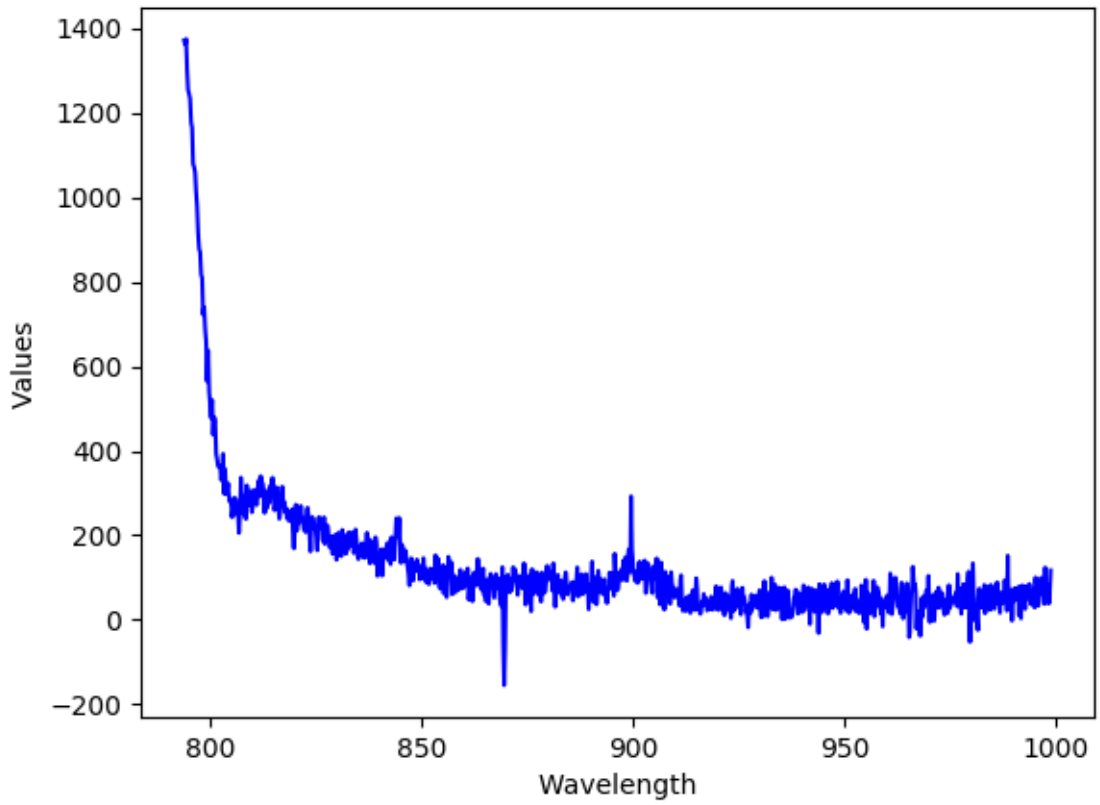

Figure 16: Raman spectra of a 2% HAc standard solution in water.

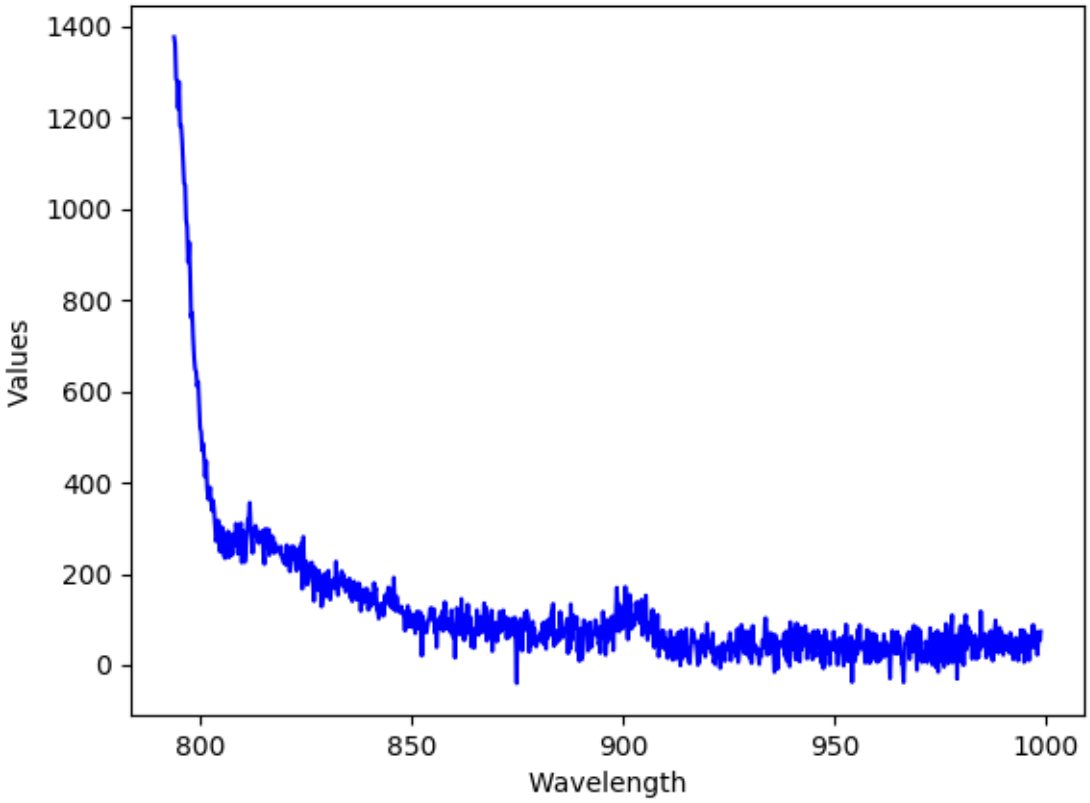

Figure 17: Raman spectra of an 1% HAc standard solution in water.

Compared to the measurement of the known concentrations the online measurements contained more noise, fig. (18) and (19). On these measurements no peaks which stood out significantly were observed. Each experimental run accumulated up to 140 Raman measurements of the anode outlet, the same trend could be observed on the others.

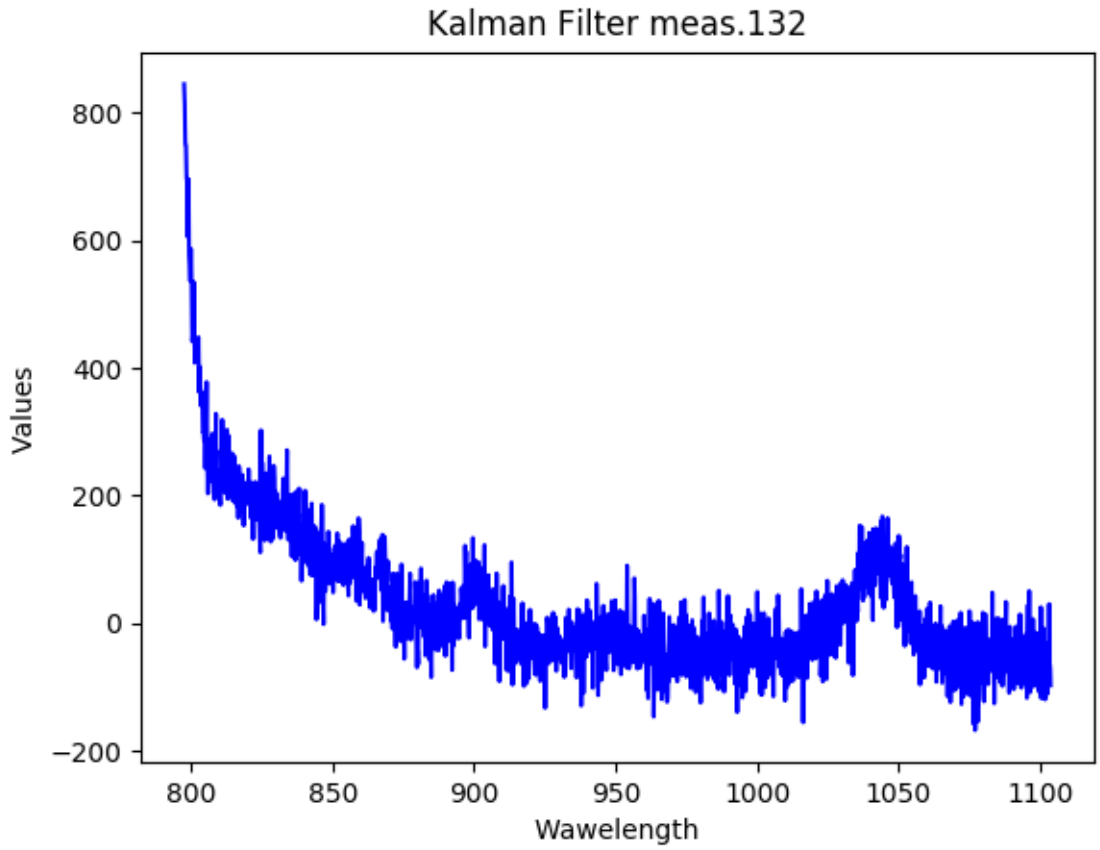

Figure 18: Raman spectra of the anolyte at the membrane outlet at 4 hours with an original 0.5% HAc solution in the cathode and 0.5A.

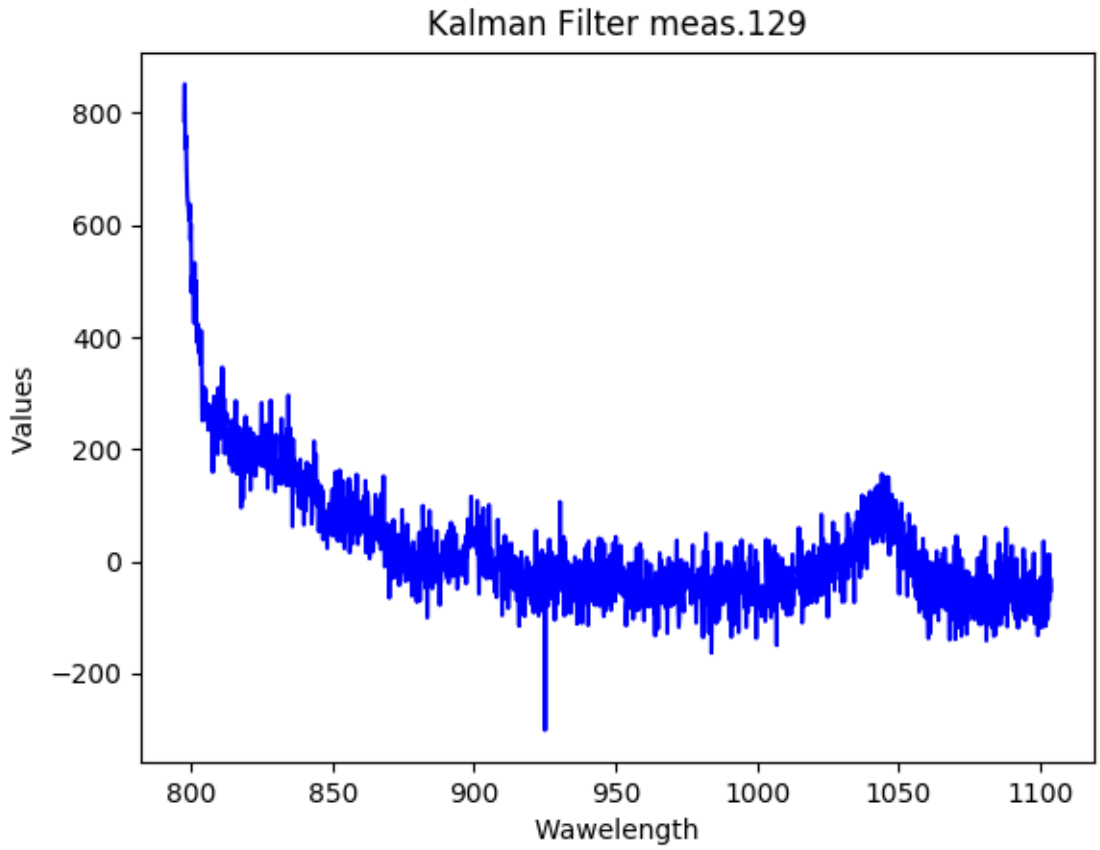

Figure 19: Raman spectra of the anolyte at the membrane outlet at 4 hours with an original 1% HAc solution in the cathode and 0.5A.

4.4 Coulombic efficiencies and mass conservation

During the 4 hours the experiments were running no changes in the liquid level were seen before and after the experiments. From the HPLC data the mass balances added up to a reasonable level except the first, 3 and the 6. experiment. The Coulombic efficiency varied if the anode was used as a source of data or the difference for the cathode. The difference can be seen in tab. (6).

Table 6: The total mass after in both compartments after 4 hours, its difference to the starting value, the coloumbic efficiencies from changes in concentrations in the cathode and anode compartments.

Run	Mass balance [g/L]	Difference to inlet [g/L]	Coulombic efficiency cathode	Coulombic efficiency anode
1	6.66	7.00	1.18	0.40
2	5.53	1.58	0.56	0.39
3	13.53	-4.97	-0.00	0.55
4	13.46	0.20	0.55	0.53
5	27.56	0.03	0.76	0.76
6	28.72	-0.688	0.76	0.84
7	6.84	0.18	0.57	0.32
8	7.12	0.15	0.51	0.29
9	13.45	0.01	0.69	0.40
10	14.22	0.29	0.69	0.38
11	28.08	0.04	0.92	0.55
12	28.21	-0.38	0.8	0.52

4.5 Rate of separation

Tab. (7) shows the transport rate when both the change in the anode concentration and the cathode concentration was calculated. The 3 first experiments show a large difference between the transfer rates for anode and the cathode. This difference was also visible in the transfer times, the time needed to empty the cathode compartment of acetate. It was a difference when the measured values from the HPLC for cathode compartment was used instead of the experimental concentrations.

Table 7: Rate of separation and transfer time of all acetic acid to anolyte. Calculated from the HPLC data for the anode and cathode compartment. Both experimental and HPLC start concentrations are shown.

Transfer rate anode [g/h]	Transfer rate cathode [g/h]	Transfer time exp. anode [h]	Transfer time exp. cathode [h]	Transfer time HPLC. anode [h]	Transfer time HPLC. cathode [h]
0.9	2.6	5.6	1.9	15.4	5.2
0.9	1.3	5.8	4.0	8.2	5.6
1.2	-0.0	8.1	-2743.3	6.9	-2347.8
1.2	1.2	8.4	8.1	11.5	11.0
1.7	1.7	11.8	11.7	16.2	16.2
1.9	1.7	10.7	11.7	14.9	16.4
0.7	0.8	7.0	6.6	9.8	9.2
0.6	0.7	7.7	7.3	11.2	10.6
0.9	0.9	11.1	10.8	15.0	14.6
0.8	0.9	11.8	10.9	17.1	15.8
1.2	1.2	16.3	16.1	22.9	22.7
1.2	1.1	17.2	18.7	23.9	26.0

4.6 ANOVA

The analysis of variance showed that there was significance for all variables on the Coulombic efficiency calculated for the anode, tab. (8). For the anode all factors had an influence. No significance could be traced for the variables to have any influence on the yield.

The rate of separation and the end time for both the original and the HPLC concentration was significant for all calculations involving the anode data. None of the cathode data showed any significance.

Table 8: Analysis of variance for the Coulombic efficiency, yield, rate of separation and fastest endtime. The independent variables were the electrical current, the concentration and the interaction between them.

Analysis of variance						
	Source	DF	Adj SS	Adj MS	F-Value	P-Value
Coulombic efficiency cathode	Concentration	2	0.22605	0.11302	1.92	0.226

	Electrical current	1	0.01068	0.01068	0.18	0.685
	Concentration* Electrical current	2	0.2796	0.1398	2.38	0.174
	Error	6	0.35271	0.05878		
	Total	11	0.86903			
Coulombic efficiency anode	Concentration	2	0.207932	0.103966	130.87	0
	Electrical current	1	0.083593	0.083593	105.23	0
	Concentration* Electrical current	2	0.016116	0.008058	10.14	0.012
	Error	6	0.004766	0.000794		
	Total	11	0.312409			
Yield	Concentration	2	0.06325	0.031623	3.5	0.099
	Electrical current	1	0.02796	0.027964	3.09	0.129
	Concentration* Electrical current	2	0.02486	0.012431	1.37	0.323
	Error	6	0.05428	0.009047		
	Total	11	0.17036			
Rate of separation anode	Concentration	2	1.0421	0.521051	130.87	0
	Electrical current	1	0.41895	0.418947	105.23	0
	Concentration* Electrical current	2	0.08077	0.040385	10.14	0.012
	Error	6	0.02389	0.003981		
	Total	11	1.56571			
Rate of separation cathode	Concentration	2	1.0207	0.5104	1.76	0.25
	Electrical current	1	0.7183	0.7183	2.48	0.166
	Concentration* Electrical current	2	1.1817	0.5909	2.04	0.211
	Error	6	1.7368	0.2895		
	Total	11	4.6575			
Endtime anode orig. conc.	Concentration	2	110.926	55.463	198.95	0
	Electrical current	1	35.512	35.5124	127.38	0
	Concentration* Electrical current	2	7.556	3.778	13.55	0.006
	Error	6	1.673	0.2788		
	Total	11	155.667			
Endtime cathode orig. conc.	Concentration	2	1262965	631482	1	0.422
	Electrical current	1	642284	642284	1.02	0.352

	Concentration* Electrical current	2	1257831	628915	1	0.423
	Error	6	3785124	630854		
	Total	11	6948204			
Endtime HPLC anode	Concentration	2	157.77	78.885	11.61	0.009
	Electrical current	1	59.32	59.319	8.73	0.025
	Concentration* Electrical current	2	49.86	24.93	3.67	0.091
	Error	6	40.77	6.795		
	Total	11	307.72			
Endtime HPLC cathode	Concentration	2	930478	465239	1	0.421
	Electrical current	1	476897	476897	1.03	0.35
	Concentration* Electrical current	2	924039	462020	1	0.423
	Error	6	2782186	463698		
	Total	11	5113600			

The contour plots for the Coulombic efficiencies showed by using the anode data fig. (20), that the highest efficiency could be achieved in the area close to 0.5 A and 2% acetate. For the data from the cathode fig. (21) a depression in the middle caused the maximum achievable efficiencies to be attained opposite to each other.

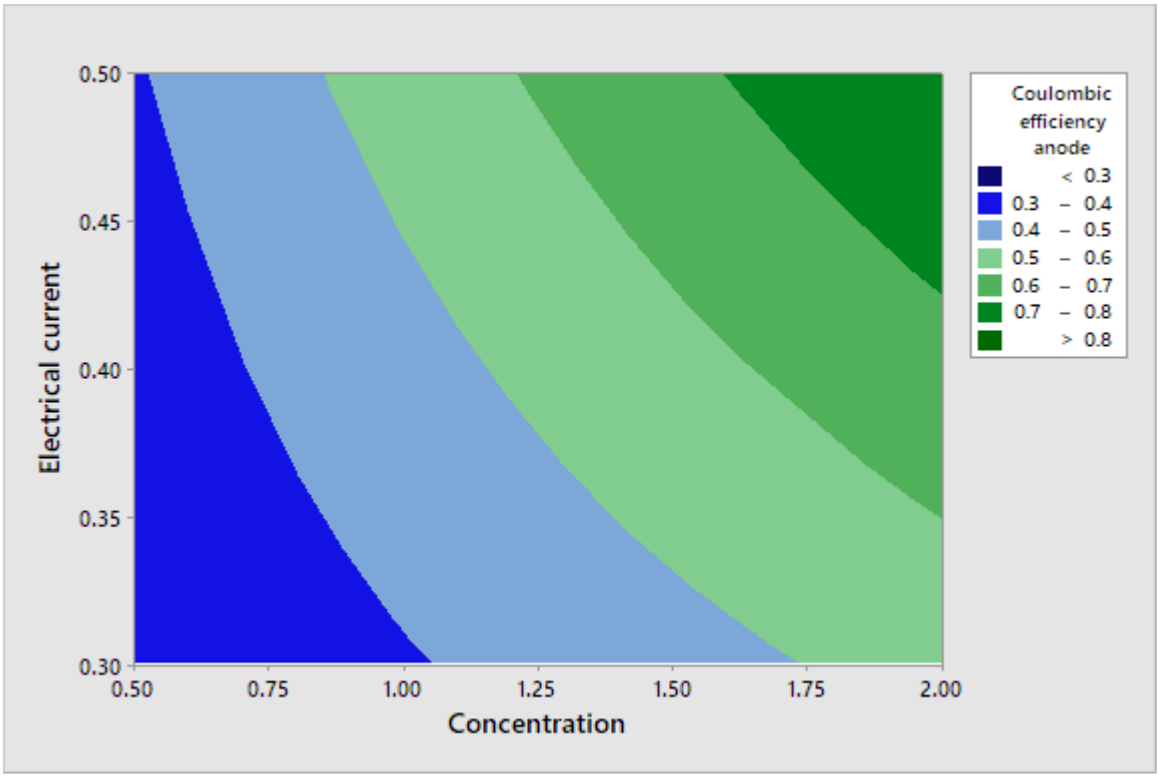

Figure 20: Contour plot of Coulombic efficiency as a function of concentration and electrical current calculated for the anode data.

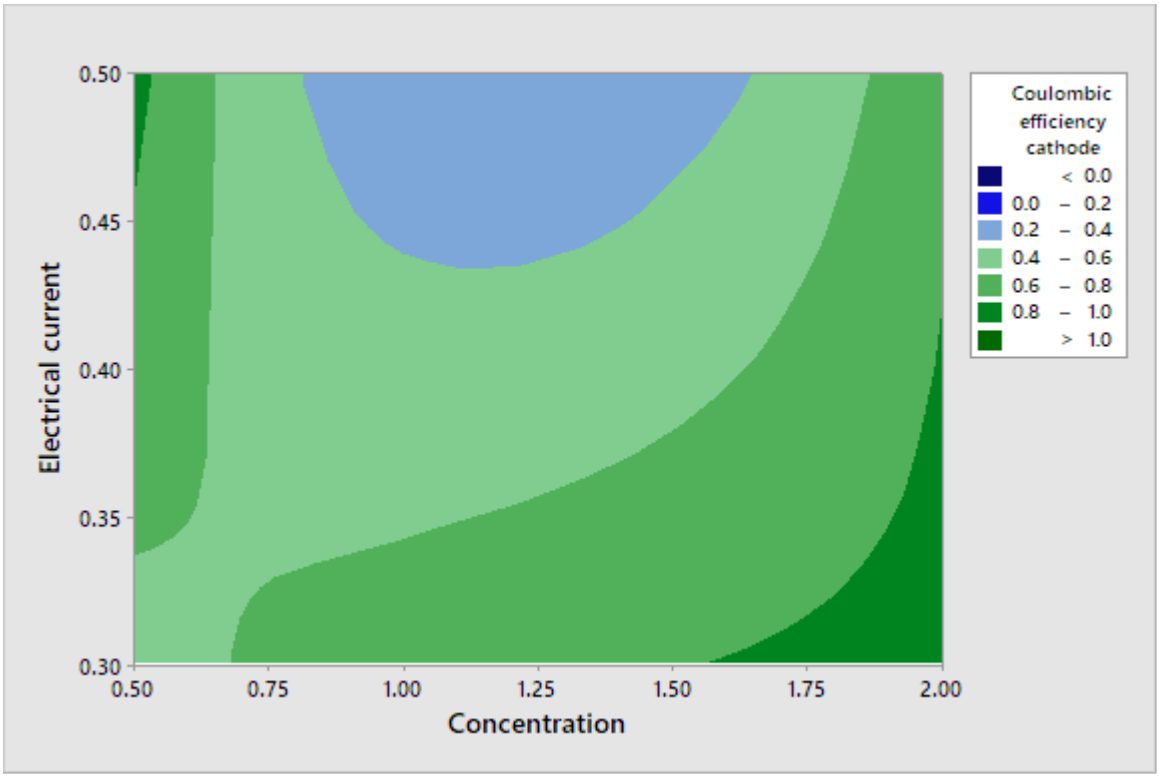

Figure 21: Contour plot of Coulombic efficiency as a function of concentration and electrical current calculated for the cathode data.

The maximum yield could be achieved close to 0.5 A and at low concentrations between 0.5 and 1%, fig. (22).

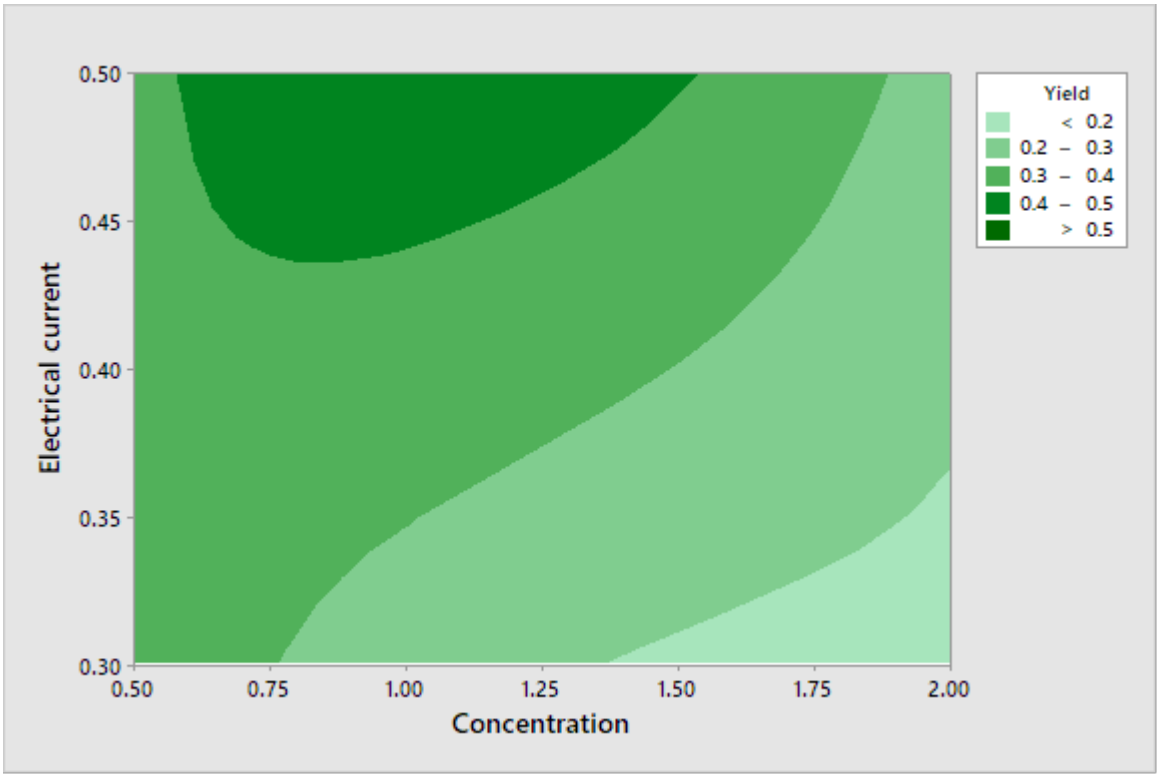

Figure 22: Contour plot of the yield as a function of concentration and electrical current.

The rate of removal was at the highest at a concentration of 2% and with an electrical current of 0.5A, fig. (23). The shortest time for complete removal was achieved by the lowest concentration and the highest current fig. (24).

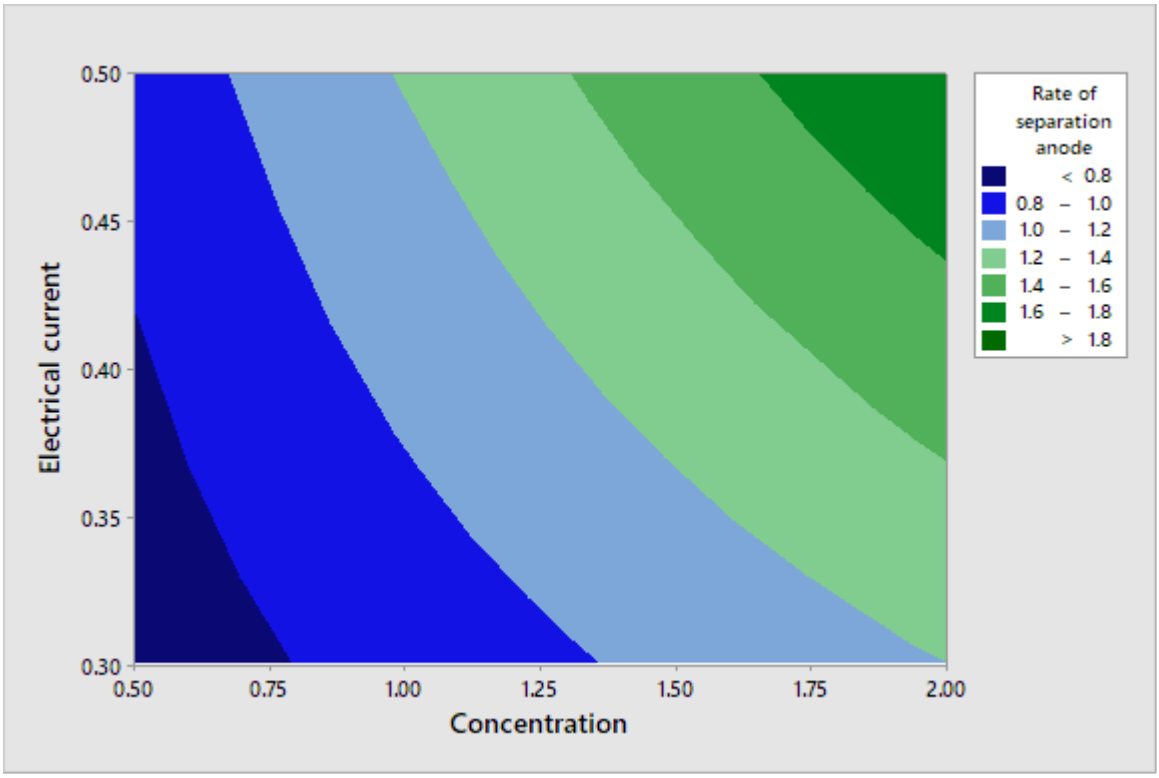

Figure 23: Contour plot for the rate of acetate removal as a function of concentration and electrical current.

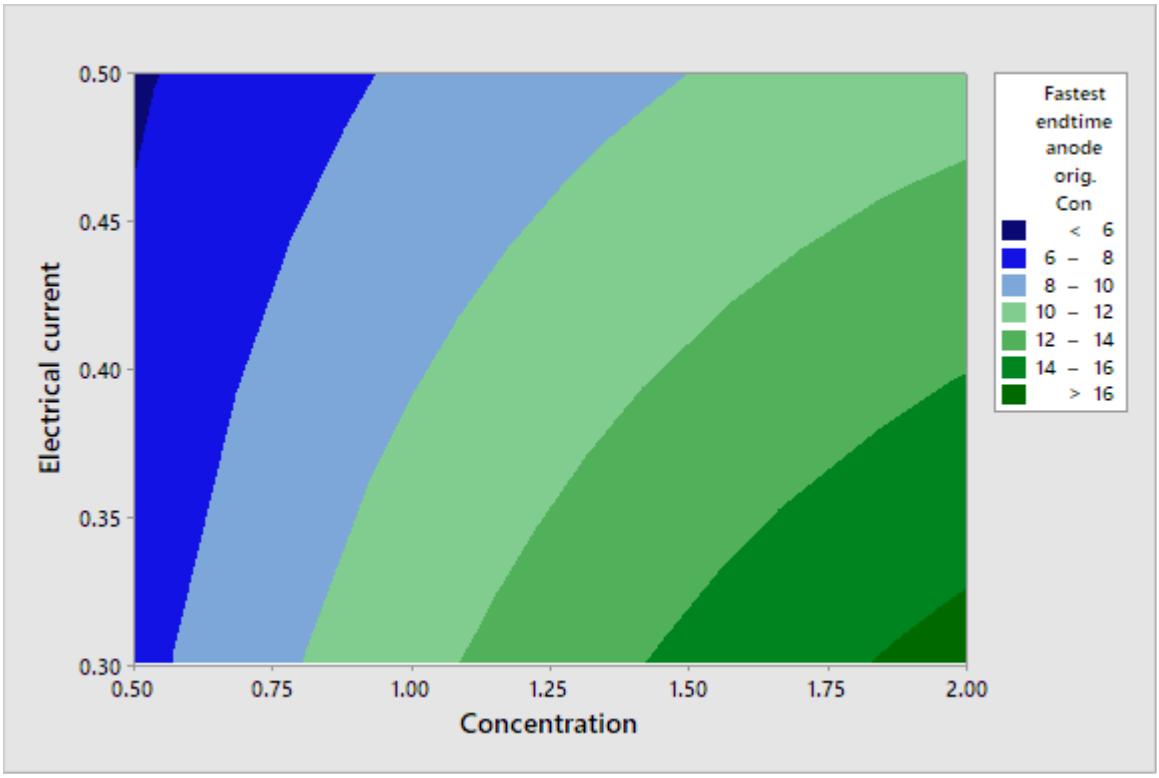

Figure 24: Contour plot for fastest possible acetate removal time as a function of concentration and electrical current for the concentrations from the experimental design.

5 Discussion

5.1 Change in temperature

The temperature increase in the system was most probably caused by the electrical resistance in the liquid. The energy supplied to the system in the form of heat is larger than the heat transferred to the environment.When liquids are returned to the fermentation reactor, the added heat can possibly offset the ideal temperature for the reactions, a cooling system could be necessary to control the ideal temperature. The heat is also an indication that not all the energy is used for the separation or the electrolysis of water.

The cathode tubing was significantly longer than the tubing of the anode. This gives the catholyte a greater surface area to lose heat after leaving the membrane. When comparing the initial concentrations in the anode and cathode compartments, the concentration of a 0.5% acetic acid solution is almost ten times higher than that of the anode. The added 2.5 mL of 100% acetic acid would give approximately 0.044 moles while the sulphuric acid supplied 0.005 moles. Lower concentrations of ions lead to a greater electrical resistance and more heat transferred to the liquid.

5.2 Discolouration of the anolyte

The change in colour was probably caused by some substance being dissolved on the anode side of the membrane. In experiments which did not achieve separation, this was not observed. In those experiments the pH on the anode side was equal to the successful experiments. As no discolouration was observed on the cathode side, it is possible that it could only be dissolved by acetic acid at a low pH. Acetic acid is a too weak acid to corrode the electrodes and since it did not happen with sulphuric acid alone in the liquid at the same pH this is unlikely. A reaction between the rubber and the acetic acid is unlikely. Because rubber is normally unreactive, a reaction with the rubber would probably increase the chance for leakages through the rubber layers, this was not observed.

5.3 Raman spectrometry

The Raman spectrometer was able to detect acetic acid within the wavelengths it operated in. The concentrations in the experiments were unfortunately lower than what the spectrometer could detect compared to the noise. To have used a higher integration time would have increased the noise correspondingly.

The increased noise level for the online measurements could have been caused by a decreased liquid level at the spectrometer. The low liquid throughput at 80 rpm could have left the tip of the spectrometer partially above the liquid and disturbed the measurement. A higher throughput would have caused a leakage in the membrane because of hydrostatic pressure difference, by how the setup was designed. On the anode the oxygen produced on the electrode had to leave the membrane alongside the liquid, making bubbles. These bubbles could have been a factor for increased noise production. As the wavelength of the peak was known the correct analysis tool could have separated the correct peak. This was not the main goal of this thesis.

5.4 Change in electrical potential

All runs showed, except run 7, that the change in electrical potential could be described by linear regression, tab. (9). Run 7 contained alongside run 1 and 3 fewer degrees of freedom than the runs with online measurements. The R-squared values indicated a lack of fit in several runs, run 4 is especially noteworthy, (30). Because of the large number of measurements run 4 still had a good probability value. All experimental runs with a concentration of 0.5% and independently of the electrical current showed a decrease in electrical potential over time. At higher concentrations an increase was observed. This can be seen for run 4 for as well during the first three hours. At higher concentrations, the concentration gradient across the membrane could have decreased faster over time than at lower concentrations, creating the need for a larger driving force supplied by the electrical potential. The experimental runs using a 2% solution had a steeper slope than their counterparts at the same electrical current.

In fig. (12) and (13) the steep decrease of the electrical potential was

caused by the liquid entering the membrane and thereby increasing the conductivity. As the current passed through the entire electrode surface, the best conductivity was achieved when the liquid level was at maximum. In fig. (12) the current was increasing at the start until it reached the setpoint.

5.5 Change in pH

During all the experimental runs the pH remained constant in the anode compartment. Because of the production of H^+ on the anode, the pH is expected to decrease slightly. The acetate ions crossing the membrane were involved in neutralizing the surplus acid. At pH 2 the concentration of H^+ was high compared to the catholyte and would need a greater change in concentration to affect the pH. The catholyte, on the other hand showed the resemblance to a buffer curve. The pka value of acetic acid is 4.76 at room temperature and at a starting pH of 8 is well outside the buffer zone. This makes a change in pH happen rapidly. To keep the charge balance, the catholyte received OH^- ions. The catholyte side had no ions with any acidic properties, thus the increase. In experiments using lactate a similar change in the pH of the catholyte has been observed as electric charge was transferred to the system (Saxena et al., 2007)

The experimental setup was not designed to measure the gas production from the electrodes. That not all the charges from the power source supplied the production of hydrogen and oxygen is likely. The electrical potential was higher than what was required to make it thermodynamically feasible. The sources of the resistance could be from the membrane and its concentration gradients, the resistance in the liquid or from water dissociation. It is likely that water dissociation was occurring due to the high value of the electrical potential. It has been reported that the limiting current density could be observed for NaCl at above 0.2 V (Strathmann, 2004a). Therefore both water splitting and dissociation could have influenced the pH.

At higher concentrations and an electrical current of 0.5A, the pH reached a steady state faster. The higher current produced a greater quantity of ions having an effect on the pH. The 0.5% and 0.5A solutions had because of the faster removal of acetate due to the current less alkalinity during the first hour. At pH 12.5 the gradient between the compartments could have caused the protons or the hydroxide ions to cross the membrane.

From the data obtained from the experiments no clear connection between the change in pH and the separation was found.

5.6 Mass balance

Since the liquid levels remained constant in all experiments the losses from evaporation can be considered negligible. If evaporation happened to a larger degree water would have been the component evaporating at the greatest extent. It has a lower boiling point, and acetic acid had a much lower molar fraction thereby reducing the possible equilibrium partial pressure. Most of the acetic acid was present in the catholyte where it exited as acetate with a much higher boiling point than its conjugate acid.

The HPLC returned values greater than what should be expected since all the mass balances had a higher concentration than what was initially added. In tab. (6) all experiments except 1, 2, 3 and 6 showed a small difference between the inlet and outlet concentrations. This indicates consistency in the results.

There was no significance by any variable on the size of the yield. Since the anova showed no significance it is problematic to interpret the validity of the yield contour plot, fig. (22). It could have been assumed that at lower concentrations the yield would have been significantly higher, this is because the current should have been able to transport a greater part of the ions.

5.7 Coulombic efficiency

Due to values outside the expected range of values for Coulombic efficiency, in addition to calculating it for the change in the cathode concentration a new calculation was done for the anode. The anode had on average a lower efficiency than the cathode even when the extreme values had been removed. One reason could be the use of the data from the HPLC giving the cathode a higher starting concentration. For both methods, there were only small differences between the replicas.

The ANOVA showed that the efficiencies calculated from the anode were significantly influenced by the experimental variables. The cathode data had

several data points that did not fulfil the need of mass conservation. Due to the low number of data points the effect of removing them, thus losing degrees of freedom was not the most viable option. Since the anode proved more consistent, its data was used to make the contour plots. If the trend in fig. (20) continued outside the experimental boundaries, the efficiency could increase with a higher current. As the concentration in a fermentation system is unlikely to increase the achievable efficiency too could be limited. This resistance was found after four hours, as the time needed for a complete separation would be longer, and the resistance increased over time, it might be unfavourable for a longer operational time. As the electrical resistance was lower at this point, it would be a favourable operating area and new experiments would likely be beneficial in this area.

5.8 Transfer rate and minimum transfer time

To check for the development of yield and mass transfer outside of the expected experimental time range, the transfer rate was calculated for both the anode and cathode. This value was the slope of the changes in concentration seen in run (11) to (10). As could be seen from the Coulombic efficiencies and mass balances, the transfer rate was unreliable for some certain points. Where the mass balances were consistent small differences could be seen between the cathode and anode calculation. If the transfer rate remained constant during the experiment it was possible to calculate the shortest time needed for 100% separation. As expected the membrane would use less time to separate if the experimental concentrations were used compared to the HPLC. The difference in the values for each experimental run was similar in the cathode and anode calculation. The large negative values should be disregarded as the replica is consistent with the pattern of the other experiments. The lowest transfer time would in all regards be regarded as unachievable as the transfer rate would most probably behave dynamically and the concentration gradient would be too high stopping a complete separation. An ideal removal time could have been calculated by using the current efficiency and assuming 100% efficiency (personal communication, Kristof Verbeeck, 29.05.2017, e-mail). This approach neglects any gradients, assuming a full separation was possible, and losses. This approach would have been less conservative than the one used, it can be applied before an experiment to find a minimum value of the removal time.

All factors had an influence on both the rate of separation and time of acetate removal. When the original concentration was used as a basis for the calculation instead of the HPLC data, the interaction had an influence. The interaction was only a tendency for the HPLC data, this could mainly be caused the first data points which did not fully correspond to mass conservation. The rate of separation had a maximal size at the highest concentration due to the size of the gradient and a higher electrical current made the transport faster, fig. (23). The acetate removal time was at the lowest for low concentrations and high currents, fig. (24). Since the experimental concentrations doubled between each level and the rate of separation did not the removal time could not increase proportionately.

6 Conclusion

Separation of acetate from the cathode to the anode compartment was achieved in all experiments. The two variables concentration and electrical current had an effect on the Coulombic efficiency, the mass transfer and transfer time. New experiments should be designed to closer examine the conditions close to 2% HAc and 0.5 A, probably increasing the current further and let the setup run for a longer time. The HPLC data from the anode showed itself in this case to more reliable for the anode. The supplied electrical current caused the liquid to heat up by two or more degrees Celsius. The electrical potential showed different behaviour over time depending on if it was the lowest concentration or the two others. The lowest concentration showed a decrease in electrical resistance during the experimental run while for higher concentrations the opposite occurred. The development of the pH was dependent on the concentration and electrical current, but showed no indication of the degree of separation.

References

Alberty, R. A. (2002). Use of legendre transforms in chemical thermodynamics: International union of pure and applied chemistry, physical chemistry division, commission on thermodynamics. *The Journal of Chemical Thermodynamics*, 34(11):1787 – 1823.

Andersen, S. J., Hennebel, T., Gildemyn, S., Coma, M., Desloover, J., Berton, J., Tsukamoto, J., Stevens, C., and Rabaey, K. (2014). Electrolytic membrane extraction enables production of fine chemicals from biorefinery sidestreams. *Environmental Science & Technology*, 48(12):7135–7142. PMID: 24844669.

Birgen, C., Preisig, H. A., Wentzel, A., Markussen, S., Wittgens, B., Sarkar, U., Ganguly, A., Saha, S., and Baksi, S. (2016). Anaerobic bio-reactor modeling. In Kravanja, Z. and Bogataj, M., editors, *26th European Symposium on Computer Aided Process Engineering*, volume 38 of *Computer Aided Chemical Engineering*, pages 577 – 582. Elsevier.

Box, G., Hunter, W., and Hunter, J. (1978). *Statistics for experimenters: an introduction to design, data analysis, and model building*. Wiley series in probability and mathematical statistics: Applied probability and statistics. Wiley.

Cornel, J., Lindenberg, C., Schöll, J., and Mazzotti, M. (2012). *Raman Spectroscopy*, pages 93–103. Wiley-VCH Verlag GmbH & Co. KGaA.

Długołęcki, P., Anet, B., Metz, S. J., Nijmeijer, K., and Wessling, M. (2010). Transport limitations in ion exchange membranes at low salt concentrations. *Journal of Membrane Science*, 346(1):163 – 171.

Du, J., Lorenz, N., Beitle, R. R., and Hestekin, J. A. (2012). Application of wafer-enhanced electrodeionization in a continuous fermentation process to produce butyric acid with clostridium tyrobutyricum. *Separation Science and Technology*, 47(1):43–51.

Dydo, P. and Turek, M. (2013). Boron transport and removal using ion-exchange membranes: A critical review. *Desalination*, 310:2 – 8. Removal of Boron from Seawater, Geothermal Water and Wastewater.

Frauendorfer, E. and Hergeth, W.-D. (2017). Industrial application of raman spectroscopy for control and optimization of vinyl acetate resin polymerization. *Analytical and Bioanalytical Chemistry*, 409(3):631–636.

Larkin, P. (2011). Chapter 2 - basic principles. In Larkin, P., editor, *Infrared and Raman Spectroscopy*, pages 7 – 25. Elsevier, Oxford.

Maddox, I. S. (1989). The acetone-butanol-ethanol fermentation: Recent progress in technology. *Biotechnology and Genetic Engineering Reviews*, 7(1):189–220.

Rubinstein, I. and Zaltzman, B. (2000). Electro-osmotically induced convection at a permselective membrane. *Phys. Rev. E*, 62:2238–2251.

Rutherford, A. (2001). *Introducing Anova and Ancova: A GLM Approach*. ISM (London, England). SAGE Publications.

Saxena, A., Gohil, G. S., and Shahi, V. K. (2007). Electrochemical membrane reactor: Single-step separation and ion substitution for the recovery of lactic acid from lactate salts. *Industrial & Engineering Chemistry Research*, 46(4):1270–1276.

Stell, G. and Joslin, C. (1986). The donnan equilibrium. *Biophysical Journal*, 50(5):855 – 859.

Strathmann, H. (2004a). Assessment of electrodialysis water desalination process costs. *in Proceedings of the International Conference on Desalination Costing, Limassol, Cyprus.*

Strathmann, H. (2004b). *Ion-Exchange Membrane Separation Processes*. Membrane Science and Technology. Elsevier Science.

Tan, J. and Ryan, E. M. (2016). Computational study of electro-convection effects on dendrite growth in batteries. *Journal of Power Sources*, 323:67 – 77.

Tanaka, Y. (2012). Mass transport in a boundary layer and in an ion exchange membrane: Mechanism of concentration polarization and water dissociation. *Russian Journal of Electrochemistry*, 48(7):665–681.

TDK-Lambda, L. (2012). *User Manual TDK Lambda*. TDK-Lambda.

Tongwen, X. and Weihua, Y. (2002). Effect of cell configurations on the performance of citric acid production by a bipolar membrane electrodialysis. *Journal of Membrane Science*, 203(12):145 – 153.

Appendices

A Offline logging of experiments

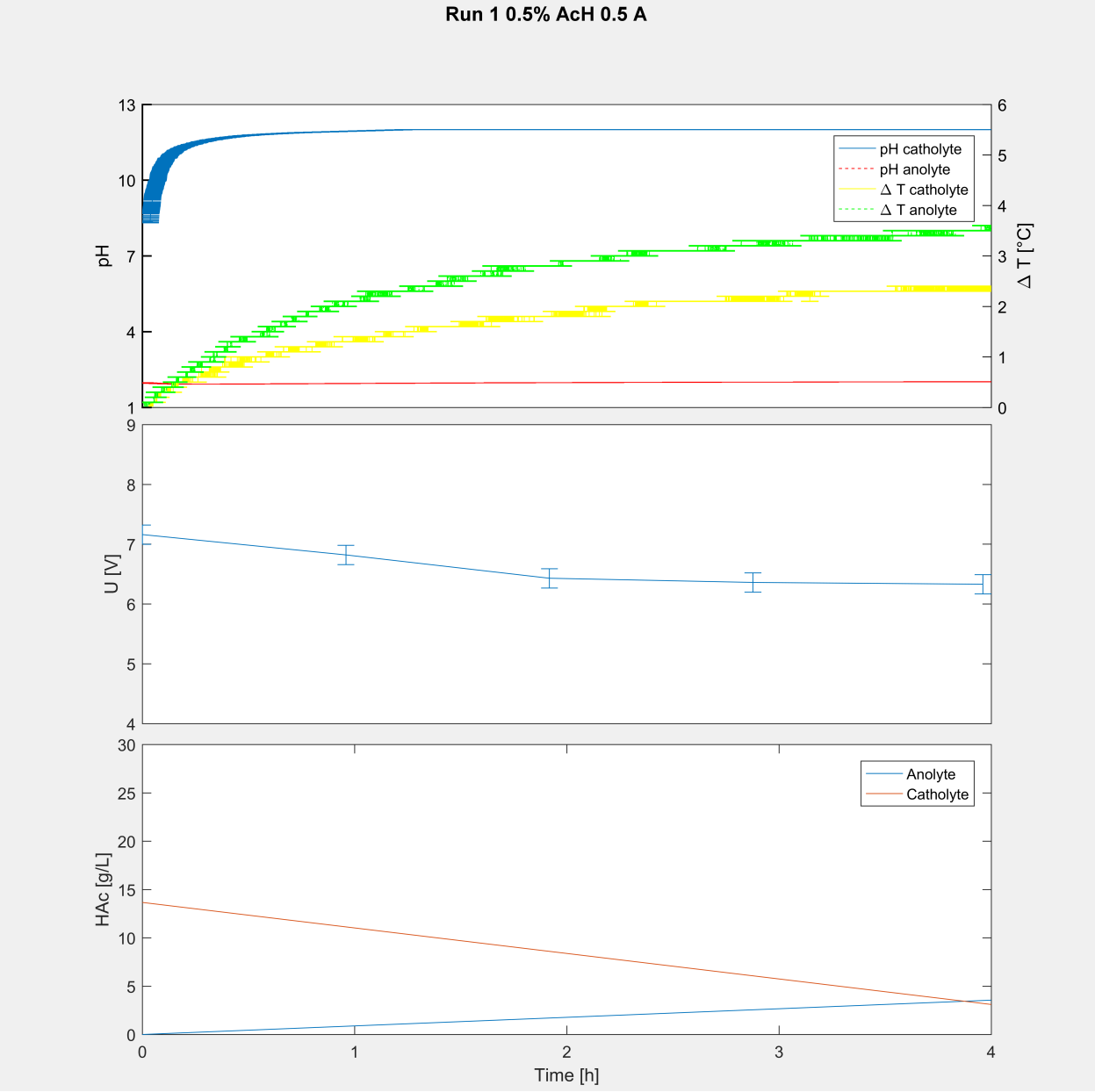

Figure 25: Development of pH, temperature, electrical potential and current and change in concentration for an experimental run using 0.5% acetate, pump speed of 80 rpm and an electrical current of 0.5 A.

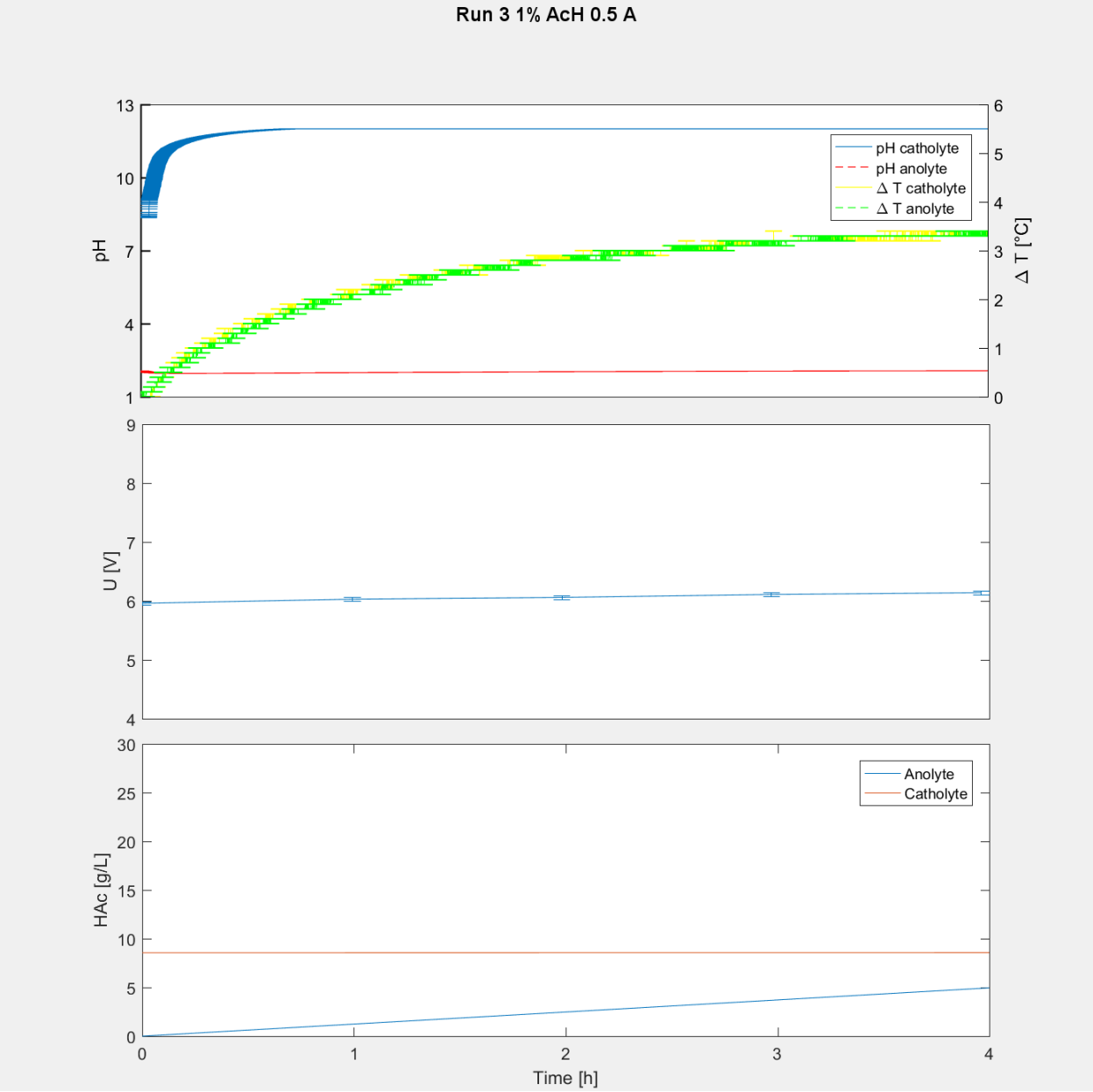

Figure 26: Development of pH, temperature, electrical potential and change in concentration for an experimental run using 1% acetate and an electrical current of 0.5 A.

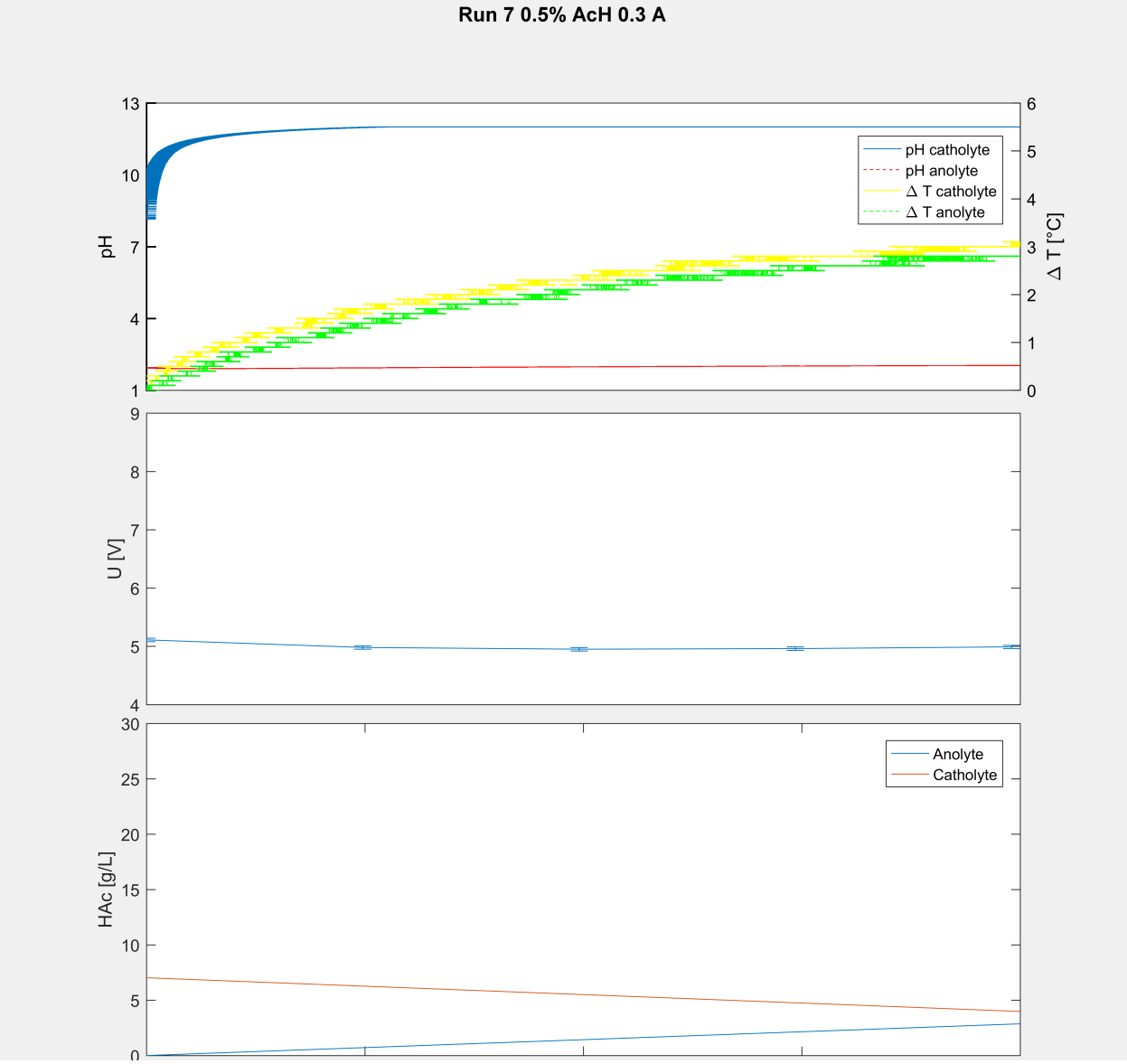

Figure 27: Development of pH, temperature, electrical potential and current and change in concentration for an experimental run using 0.5% acetate and an electrical current of 0.3 A.

B Linear regression of change in electrical potential

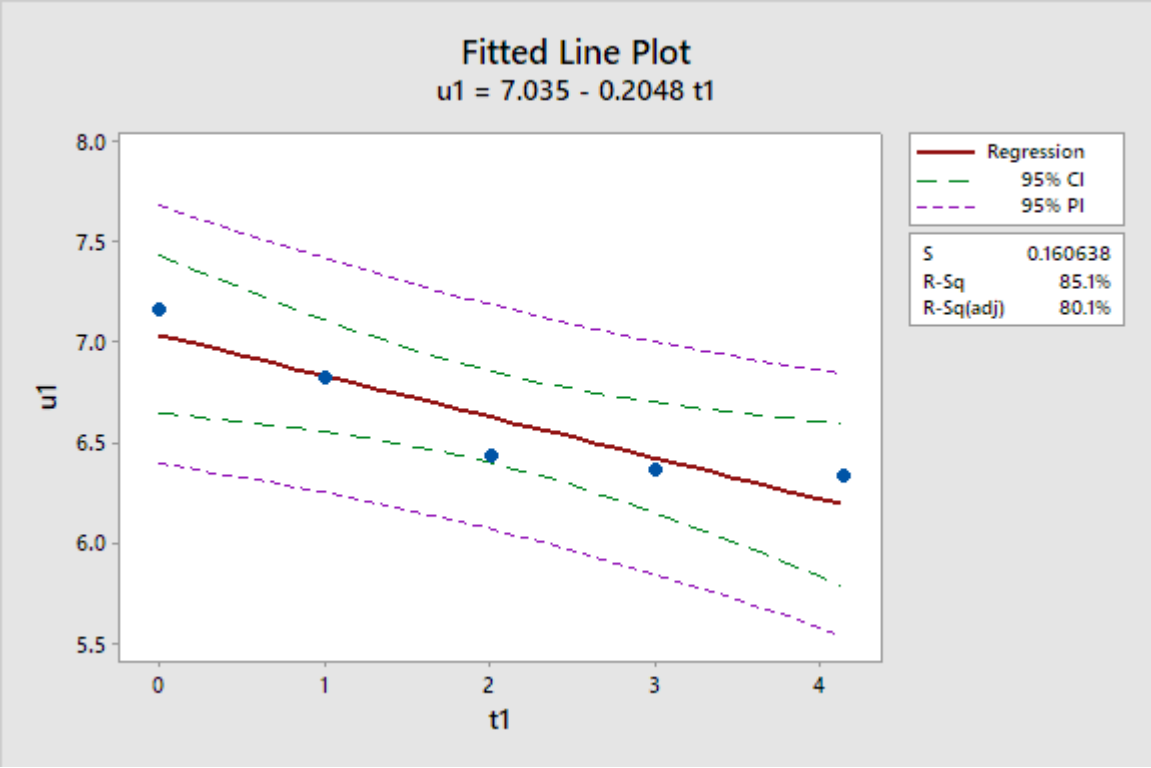

Figure 28: Linear regression plot for experimental run 1 in the 2x3 factorial experiment. Conditions are: 0.5% acetate and 0.5 A.

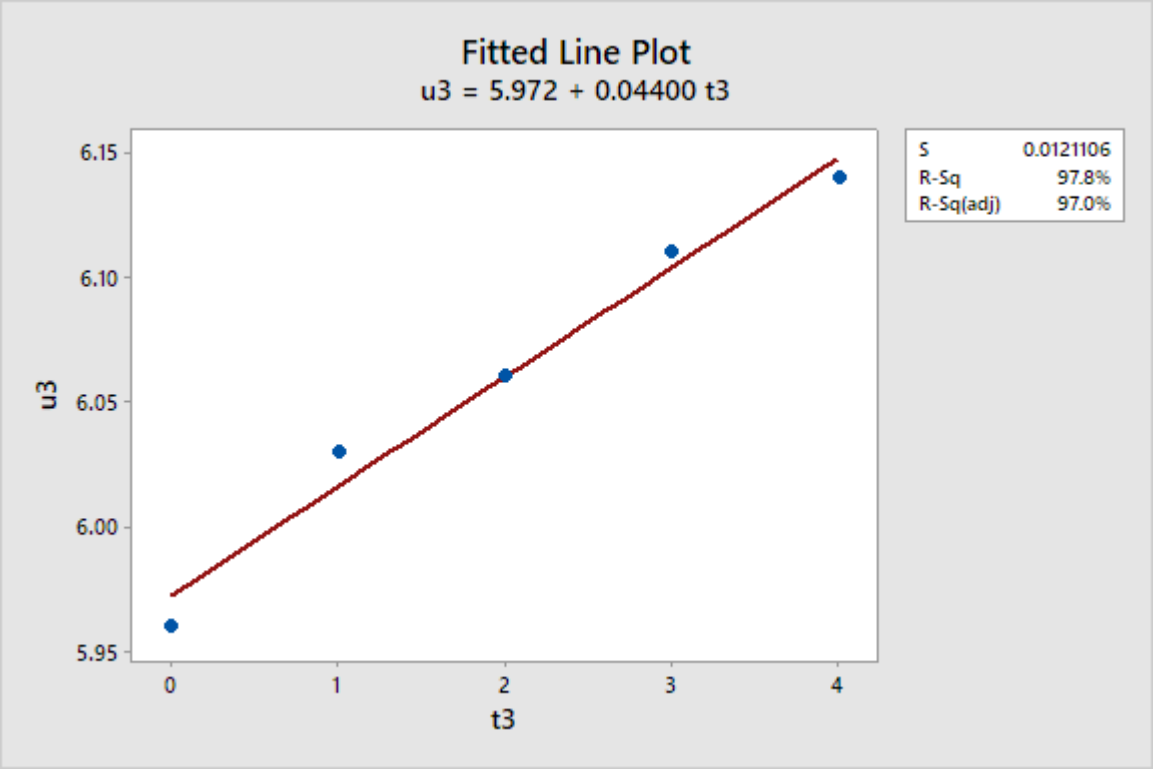

Figure 29: Linear regression plot for experimental run 3 in the 2x3 factorial experiment. Conditions are: 1% acetate and 0.5 A.

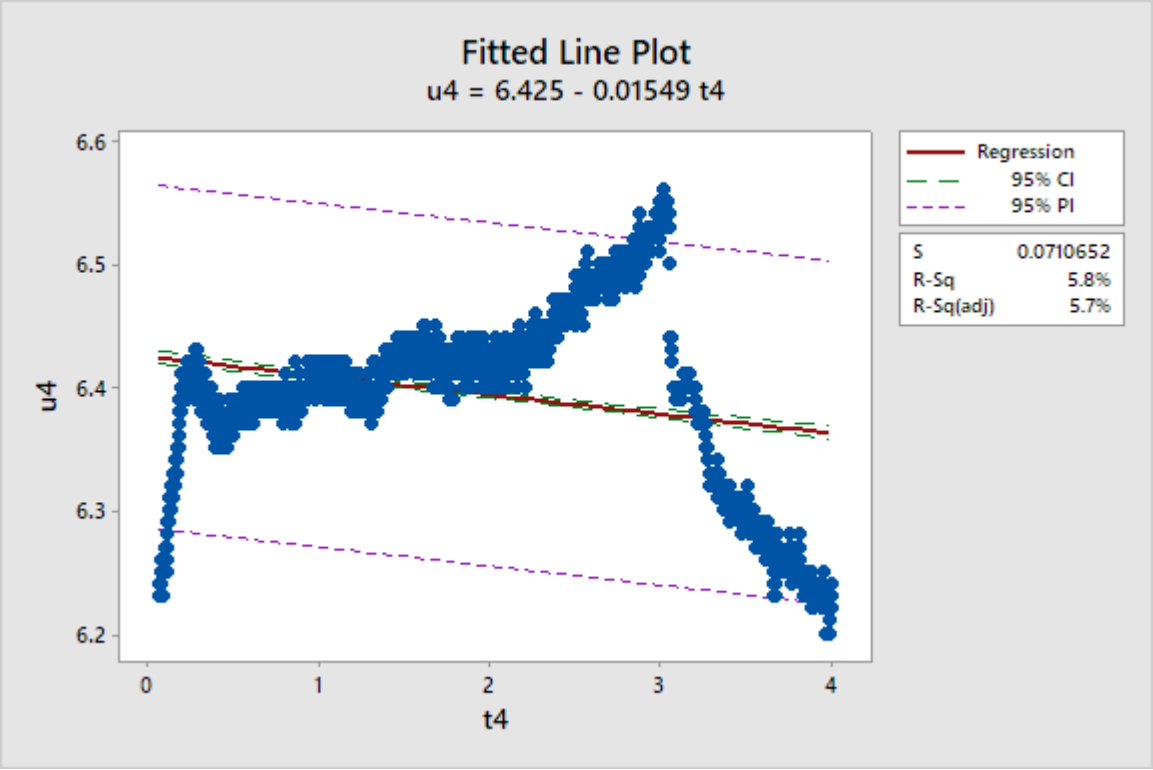

Figure 30: Linear regression plot for experimental run 4 in the 2x3 factorial experiment. Conditions are: 1% acetate and 0.5 A.

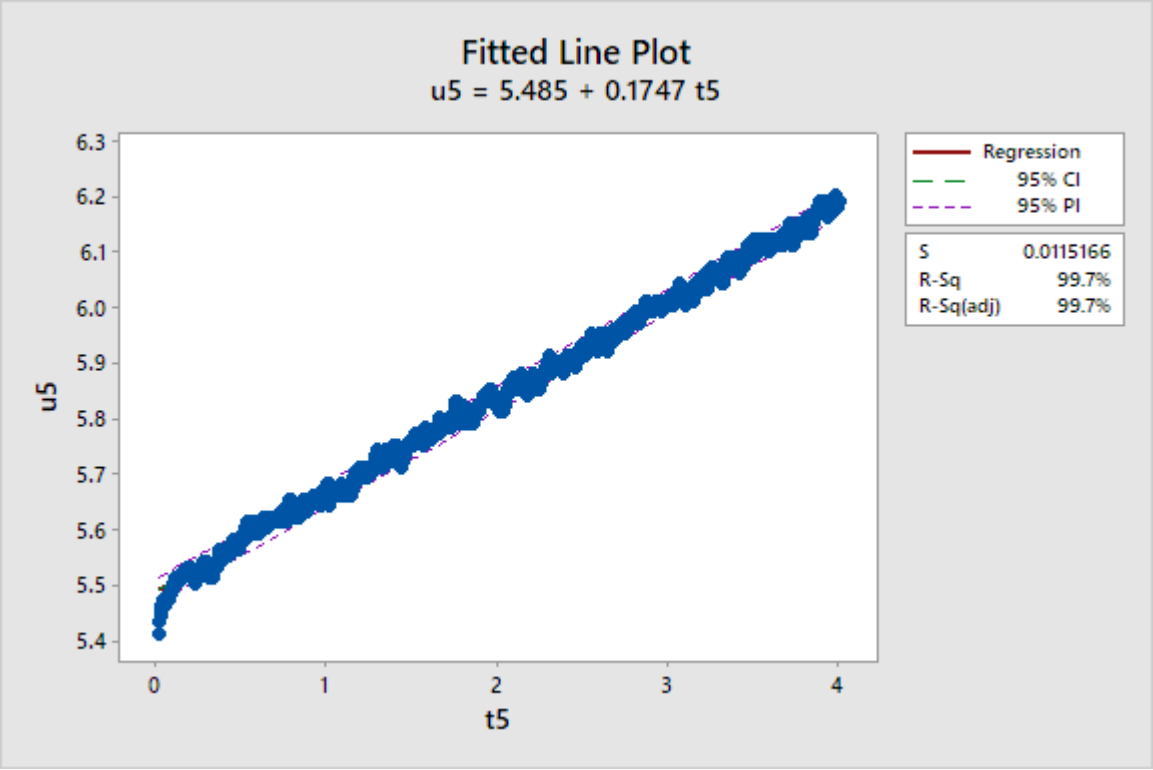

Figure 31: Linear regression plot for experimental run 5 in the 2x3 factorial experiment. Conditions are: 2% acetate and 0.5 A.

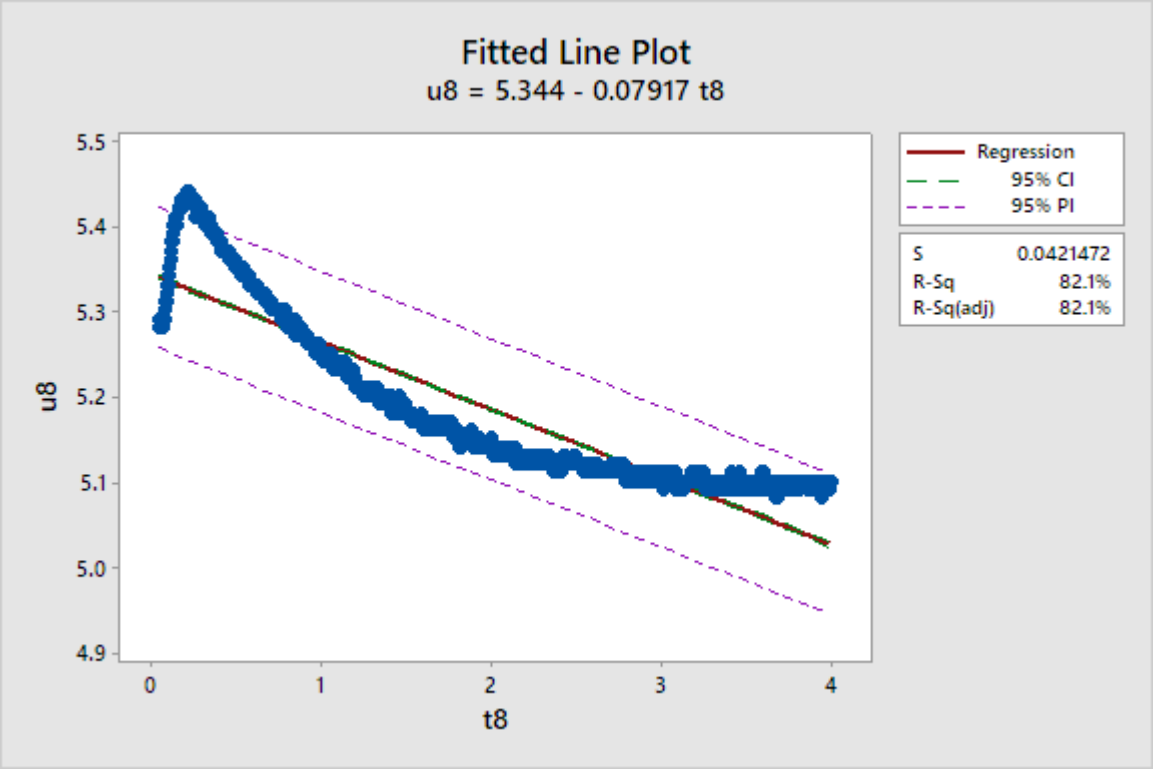

Figure 32: Linear regression plot for experimental run 8 in the 2x3 factorial experiment. Conditions are: 0.5% acetate and 0.3 A.

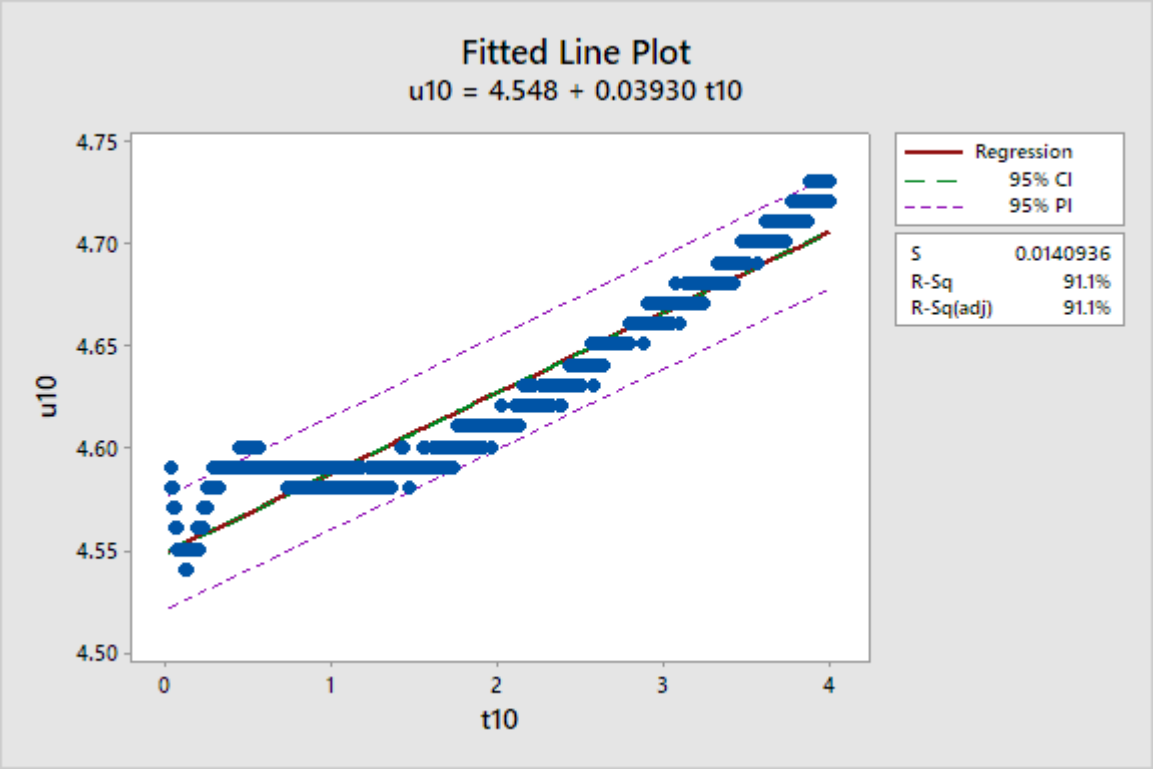

Figure 33: Linear regression plot for experimental run 10 in the 2x3 factorial experiment. Conditions are: 1% acetate and 0.3 A.

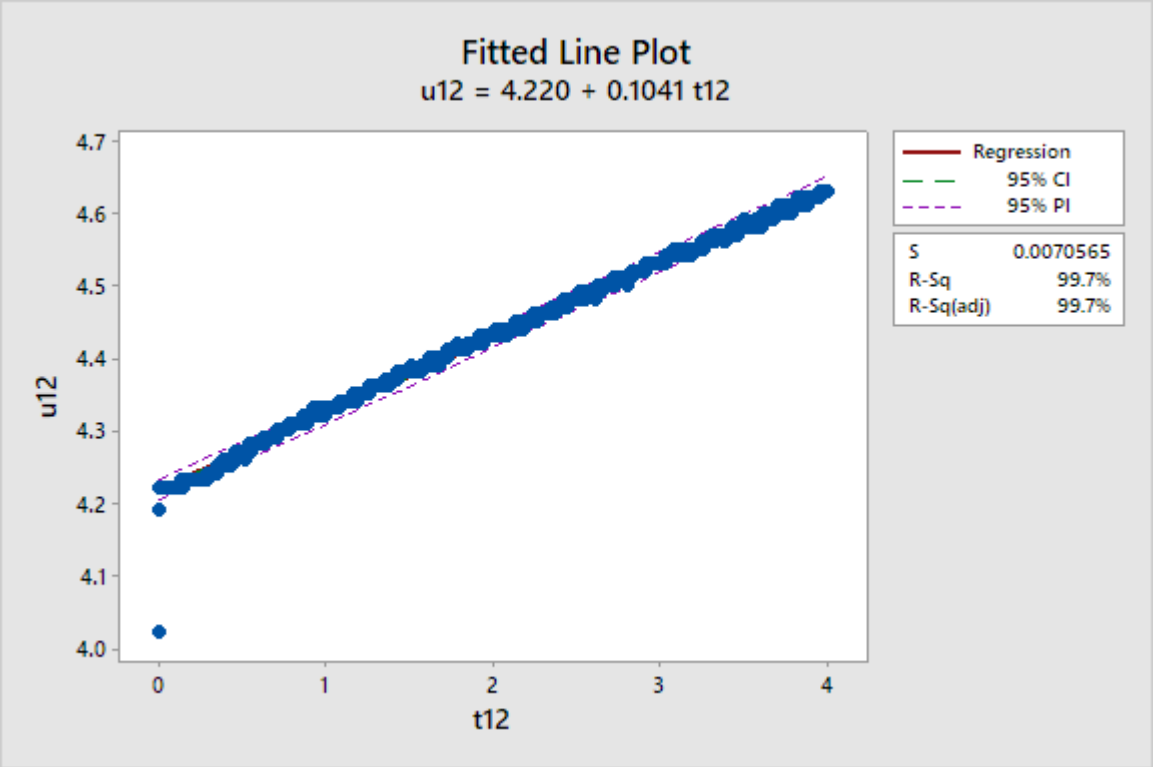

Figure 34: Linear regression plot for experimental run 12 in the 2x3 factorial experiment. Conditions are: 2% acetate and 0.3 A.

Table 9: Analysis of variance for the linear regression of 12 experiments in the experimental run.

Analysis of variance						
	Source	DF	SS	MS	F	P
Run 1	Regression	1	0.441986	0.441986	17.13	0.026
	Error	3	0.077414	0.025805		
	Total	4	0.51940			
Run 2	Regression	1	842.48	842.482	9324.46	0.000
	Error	2789	251.99	0.090		
	Total	2790	1094.47			
Run 3	Regression	1	0.01936	0.0193600	132.00	0.001
	Error	3	0.00044	0.0001467		
	Total	4	0.01980			

	Regression	1	0.8485	0.848495	168.01	0.000
Run 4	Error	2741	13.8428	0.005050		
	Total	2742	14.6913			
	Regression	1	111.668	111.668	841942.53	0.000
Run 5	Error	2773	0.368	0.000		
	Total	2774	112.036			
	Regression	1	107.463	107.463	203849.78	0.000
Run 6	Error	2787	1.469	0.001		
	Total	2788	108.932			
	Regression	1	0.00676	0.0067600	2.04	0.248
Run 7	Error	3	0.00992	0.0033067		
	Total	4	0.01668			
	Regression	1	22.4587	22.4587	12642.93	0.000
Run 8	Error	2754	4.8922	0.0018		
	Total	2755	27.3509			
	Regression	1	1.86155	1.86155	6370.17	0.000
Run 9	Error	2768	0.80889	0.00029		
	Total	2769	2.67044			
	Regression	1	5.62751	5.62751	28331.58	0.000
Run 10	Error	2768	0.54981	0.00020		
	Total	2769	6.17732			
	Regression	1	42.4426	42.4426	268359.65	0.000
Run 11	Error	2749	0.4348	0.0002		
	Total	2750	42.8773			
	Regression	1	40.3146	40.3146	809614.27	0.000
Run 12	Error	2788	0.1388	0.0000		
	Total	2789	40.4535			